

Separation Train Design and Optimization in Offshore Oil and Gas Production Facilities

Suborna Rani Nath



Masters Thesis (Short) 2022



AALBORG UNIVERSITY
STUDENT REPORT

Title: Separation Train Design and Optimization in Offshore Oil and Gas Production facilities.

Theme:

Abstract: Scientific Theme

Project Period: Autumn Semester
2022

Project Group:

K10-OG-2-F22

Participant:

Suborna Rani Nath

Supervisor(s):

Rudi P. Nielsen

Copies: 1

Number of pages: 78

Date of Completion:

August 29, 2022

The aim of this work was to build up a simulation model of separation train design for oil and gas separation in order to investigate the effect of varying operating pressure and temperature on oil and gas flow rate. The operating conditions can have a remarkable impact on the quantity of the oil and gas production and therefore maximizing the profit. The simulation is conducted using Aspen HYSYS. The simulation result showed that increasing the 1st stage pressure but decreasing the temperature the production of oil is rises. In contrast, reducing 1st stage and 2nd stage temperature oil production rises. The study represents a powerful optimization tool for the selection of optimum operating pressure and temperature values for an offshore oil and gas separation train in order to maximize the profit of oil and gas sales. Response surface methodology (RSM) was performed by subsequent construction of Multiple linear regression (MLR) model for the chosen responses to determine the optimum operating point that generates a greatest impact on profit. Multiple regression model revealed the optimum outcome of the profit function. To conclude, RSM was successfully predicted the optimum operating conditions for maximum profit that occurs at $P1 = 38.08$ bar, $T1 = 54.09^{\circ}\text{C}$, $P2 = 18.00$ bar and $T2 = 40.56^{\circ}\text{C}$ predicted at 0.208 milli. \$/day. Thus, the overall separation process optimized in terms of profit function under the constraints of 1st and 2nd stage temperature and 1st stage pressure.

Acknowledgement

This project report was done for the 10th semester at the Department of Chemical Engineering, Aalborg University, Esbjerg between February to June 2022. The project was carried out under the supervision of Professor Rudi P. Nielsen from the section of Chemical Engineering at Aalborg University, Esbjerg. The project deals with separation train design and optimization in offshore oil and gasproduction facilities.

It was a huge experience of learning in chemical engineering at Aalborg University, Esbjerg.

I would like to express my sincere gratitude and special thanks to my supervisors for sharing their knowledge, energy, and time for answering my infinite questions, giving necessary guidance and support as their student.

The project report is a collection of scientific papers. The first part of the report is an introduction describing the background for this project. This includes the extent of how big the issue is and hence, why this project work is important. The section ended with an objective section and describing goal, I set for myself from the beginning of the project.

I sincerely hope that you as readers will find my results and the project interesting.

Sincerely,

Suborna Rani Nath

Aalborg University, Esbjerg

29 August 2022

Table of Contents

Acknowledgement.....	3
Chapter 1: Introduction.....	7
Chapter 2: Crude oil, gas and reservoir fluids.....	10
2. Petroleum Reservoir fluids	10
2.1. Classification	10
2.2. Physical properties of petroleum reservoir fluids	17
2.3. Vapor pressure measurements	18
Chapter 3: Offshore oil and gas production.....	20
3. Offshore oil and gas facilities	20
3.1. Separation of Reservoir fluids	22
3.2. Summary	26
Chapter 4: Thermodynamic modelling.....	27
4. Thermodynamic Analysis	27
4.1. Flash Calculations	28
4.2. Summary	32
Chapter 5: Problem formulation.....	33
Chapter 6: Methodology.....	35
6. Experimental plan	35
6.1. Process Description	36
6.2. Objective function	41
6.3. Energy consumption	43
6.4. Optimization	44
6.5. Experimental design and statistical analysis	45
6.6. Summary	51
Chapter 7: Results and Discussion.....	52
7. Result Analysis	52
7.1. Case studies	55
7.2. Result analysis on Energy Consumption	58
7.3. Optimization result	61
Chapter 8: Conclusion and future work.....	73
8.1. Conclusion	73
8.2. Future work	74
Appendix 1:	75
References	76

List of Figures

Figure 1: Oil and gas industry (reproduced from (Pasquale, 2007))	8
Figure 2: Structure of a typical reservoir fluid well (Speight & James G, 2014).	11
Figure 3: A typical dry gas reservoir phase diagram [reproduced from (ARNOLD, 2007)].	12
Figure 4: A typical wet gas reservoir phase diagram [reproduced from (ARNOLD, 2007)].	13
Figure 5: A phase diagram of a condensate gas reservoir [reproduced from (ARNOLD, 2007)].	14
Figure 6: A phase diagram of a volatile oil reservoir [reproduced from (ARNOLD, 2007)].	14
Figure 7: A black oil reservoir phase diagram [reproduced from (ARNOLD, 2007)].	15
Figure 8: Example of Chemical Structures of Paraffins or alkanes (Pedersen & Christensen, 2007).	16
Figure 9: Example of Chemical Structures of Naphthes (Pedersen & Christensen, 2007).	16
Figure 10: Example of Chemical Structures of Aromatics (Pedersen & Christensen, 2007).	17
Figure 11: Shallow water complex offshore platform (aau student, Csanyi, 2017)	21
Figure 12: Oil and gas separation train [reproduced from (Pasquale, 2007)].	23
Figure 13: Flash tank (Becker et al., 2015).	29
Figure 14: VLE algorithm flowchart using isothermal two-phase flash calculations and the PR-EOS (Neto & Bannwart, 2015).	32
Figure 15: Experimental plan.	35
Figure 16: A schematic process flow sheet of an offshore oil and gas simulation train.	38
Figure 17: CCD model for four factors or variables X_1, X_2, X_3 and X_4 [5].	47
Figure 18: T_1 and P_1 at 60°C and 50 bar on mass flow rate of oil.	57
Figure 19: T_1 and P_1 at 60°C and 50 bar on mass flow rate of gas.	57
Figure 20: Energy consumption in C1 & C2 at $T_1=60^\circ\text{C}$ and $P_1=50$ bar.	59
Figure 21: Energy consumption in C1 & C2 at $T_1=60^\circ\text{C}$ and $P_1=50$ bar.	60
Figure 22: Correlation matrix among the variables.	62
Figure 23: Predicted vs. Actual values of profit.	64
Figure 24: Response surface for the effect of (a. T_1 and P_1 on Profit function), (b. T_2 and P_2 on profit function).	69
Figure 25: The optimum region by the saddle point in the contour plot for profit evaluated as function of (a. 1st stage pressure, $P_1= 38.08$ bar and temperature, $T_1 = 40.56^\circ\text{C}$), (b. 2nd stage pressure, $P_2=$ and temperature, $T_2 = 40.56^\circ\text{C}$).	71

List of Tables

Table 1: Physical Properties of Petroleum Reservoir Fluid Components (Hu, 2017).	17
Table 2: The standards used to produce this gas condensate specification are listed in the table below....	19
Table 3: The composition and characterization for the investigated well-fluid.	39
Table 4: Operating conditions and design parameters of the flowsheet.	40
Table 5: 24 factorial level used in central composite design (CCD).....	49
Table 6: Dependent and independent variable used to perform multiple linear regression model.....	50
Table 7: The table below gathers the process parameters that are set to meet the specifications on the crude oil and gas.....	52
Table 8: Regression model for C2 (Compressor 2).	61
Table 9: Prediction model for Multiple regression model.	63
Table 10: Regression coefficients of the second order polynomial model for the profit (actual values). ..	66
Table 11: ANOVA table of the second order polynomial model for the profit (Actual values)	66
Table 12: Regression coefficients of the second order polynomial model without two-way interaction effect for the profit (actual values of profit).....	67
Table 13: ANOVA table of the second order polynomial model without Two-way interaction model for the profit (Actual values).	68
Table 14: Process simulation responses to coded variable build using CCD. 1=high value, 0= mid value and -1= low value.	75

Chapter 1: Introduction

Offshore oil and gas production facilities are the platforms that produce transportable well stream by pipelines and tankers. A well fluid may be made up of gas, oil, and water. Separation is the process to separate the well stream into three phases (oil, gas, and water) due to the space and utility limitations at the offshore platforms. Hydrocarbon mixtures are separated through multiple separation stages at successively lower pressures (i.e., a series of flashes) so that the overall process simulates a differential (rather than a single flash) separation. The separation procedure would resemble a flash vaporization process with minimal liquid recovery if only one separator were utilized. In general, as the number of stages increases, the process resembles a real differential separation, and oil recovery is maximized (Bin Dainure, 2013). A separation train design with three stage separation process is usually the most minimal.

The performance of separating the light and intermediate components into gas and oil products to ensure maximum oil recovery is the most crucial design element of an offshore oil and gas production facility. The separator will be modelled by using phase equilibrium calculations by the means of density difference and/or progressive reduction of pressure and temperature. Therefore, a thermodynamic model must be chosen to accomplish a flash separation in each single separation stage. The thermodynamic model provides the relation between pressure, temperature and molar volume for hydrocarbons and mixtures. Since, from the reservoir to the first stage separator and between the separators a considerable amount of pressure and temperature reduction occurs. It is thus reasonable to assume that the fluid separates into a liquid and vapour phase, where the operating conditions are placed well inside the two-phase region of the separators. As this simplifies the problem forming vapour liquid equilibrium calculation (Kylling, 2009; Pasquale, 2007).

However, to achieve the process goal for a desired separation adjusting pressure and temperature is the general approach of separating liquid well fluid into the two phases to ensure

higher separation efficiency (Qadri et al., 2020). Choosing both the pressure and temperature of the sequential separators is sufficient to determine the proper design variables for maximizing the profit of oil and gas sales which is generally driven by the export quantity of crude oil. On the other hand, more contemporary approaches include the coupling of the separation and recompression trains in order to determine the values of the design variables that would maximize the profit (i. e., the sum of the profits from the sale of oil and gas minus the operating costs).

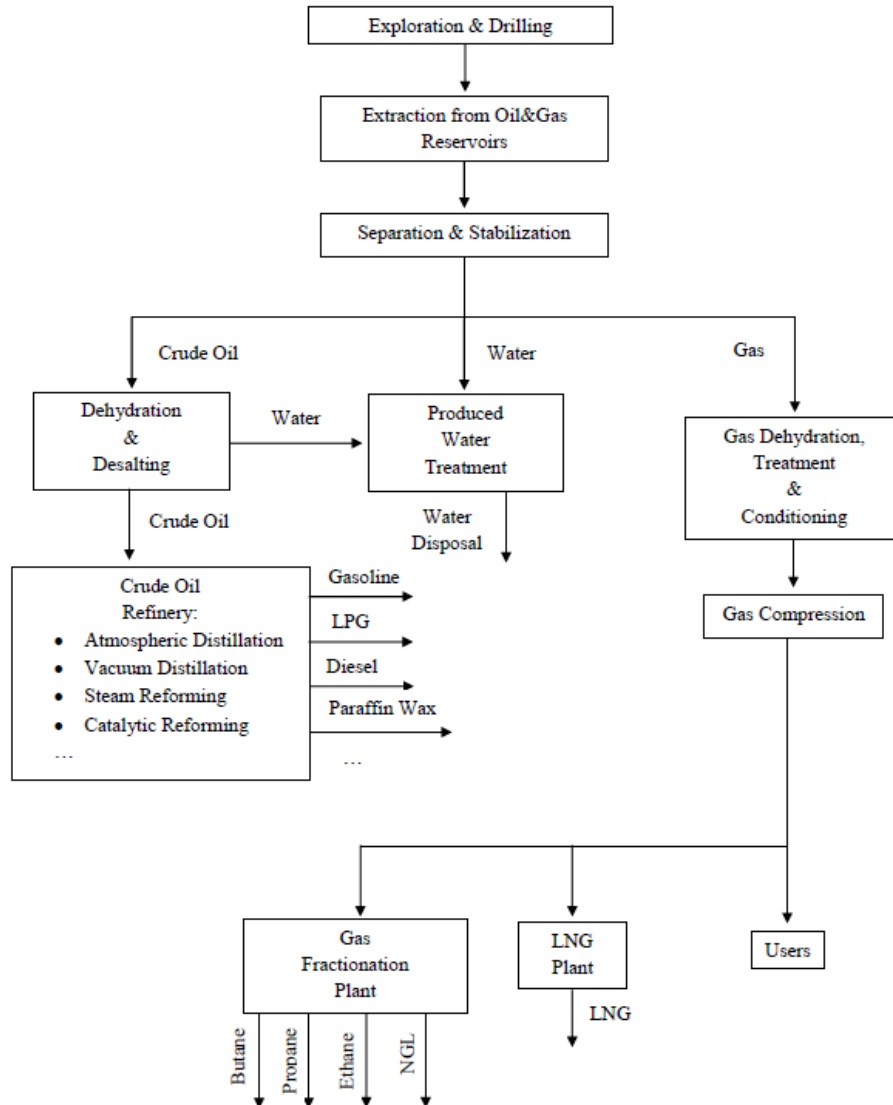


Figure 1: Oil and gas industry (reproduced from (Pasquale, 2007))

Figure 1 illustrates how the potential extraction of the hydrocarbon reservoir fluids and how they are processed to deliver various products (Pasquale, 2007).

This project report subdivided into two main sections: One section is based on theoretical overview, while the other one is investigation of the issue using simulation tools used in an offshore oil and gas plant. The theoretical section of the paper contains the most important material from the literature review for this project. The second part is to find out the optimum pressures and temperatures for maximum profit through an optimization method which maximizes the income from the crude oil and gas sales.

In this study, the optimal operating conditions for a complex and realistic oil and gas separation plant are examined with 3-stage separation, coupled with the compression train for compressing the flash gas from all separators, including condensate recycles. By simulating the separation plant using a process simulation model using Aspen HYSYS to obtain optimum operating condition i.e., maximizing the profit, is investigated, including taking into account maximizing the recovery of intermediate hydrocarbons (C_3 , C_4 , C_5) in the Crude Oil and energy consumption.

Chapter 2: Crude oil, gas and reservoir fluids

The aim of this chapter is to present an overview of the crude oil, gas and reservoir fluids, their classification, and analysing their physical properties with a focus on offshore plant.

2. Petroleum Reservoir fluids

The term “*Petroleum reservoir fluids*” are complex mixtures of thousands of constituents, primarily hydrocarbons and trace amounts of inorganic compounds, among which water, nitrogen (N_2), carbon dioxide (CO_2), hydrogen sulphide (H_2S) is the most common (Hu, 2017).

Typically, crude oil and natural gas deposits are typically discovered in porous, permeable rocks with a coarse grain that contain little or no insoluble organisms (Speight & James G, 2014). The process of petroleum formation begins with the burial of these organisms beneath layers of clay and sediments, resulting in an organic matter and clay matrix. This matrix is gradually transformed into kerogen, a new substance. With the corresponding increase of pressure and temperature kerogen will be encased deeper and deeper with the deposition of clay and sediment. Kerogen transition into oil and gas occurs over extended periods of time (millions of years) and at depths between 760 and 4900m (Pasquale, 2007).

The accumulation of oil and gas is caused by the occurrence of an impermeable barrier. Petroleum fluid begins to move laterally due to pressure differences, following the path made by permeable rocks, until it reaches dome structures known as anticlines, where it is trapped. Therefore, petroleum begins to build up over time. Crude oil constituents may move because of active water flow or either by displacement or diffusion, where water disposes in the bottom while natural gas floats on the top (Pasquale, 2007; Speight & James G, 2014).

2.1. Classification

Petroleum reservoir fluids can be categorized based on the critical temperatures of hydrocarbon multicomponent mixtures compared to the reservoir temperature. Indeed, critical temperature is

the point where the bubble and dew pressure branches meet in a phase envelope in a PT diagram. According to McCain et al. 2011, the composition of a well fluid changes, so does the critical temperature and the branches of the phase envelope changes. The following main classifications based on some thermodynamic parameters, such as pressure and temperature, and composition (Pasquale, 2007, Bidgoli, 2020):

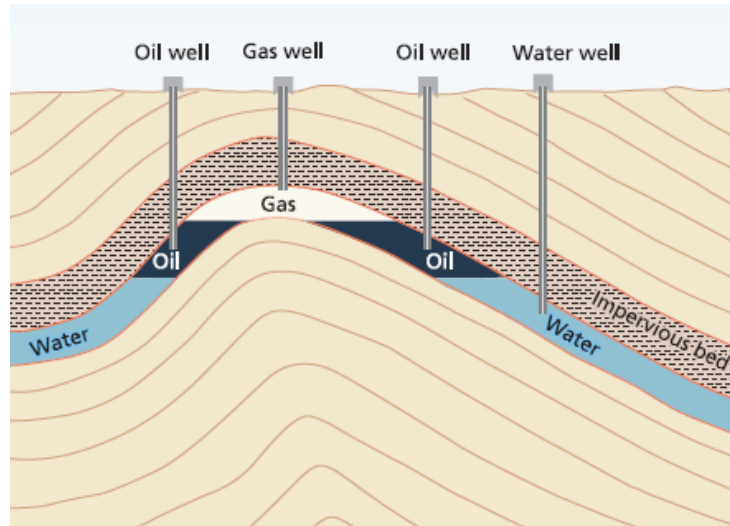


Figure 2: Structure of a typical reservoir fluid well (Speight & James G, 2014).

- **Dry gas:** As illustrated in figure 3, all hydrocarbon components are in the gas phase in the reservoir or at the surface. The term "dry" refers to the fact that this gas contains insufficient heavier components to form hydrocarbon liquid at the surface line (1→2) does not pass through the phase envelope, resulting in dry gas is mostly methane with some other intermediates. At reservoir and surface separator conditions, the pressure path only dry gas. Point 1 is in a reservoir state, while point 2 is at the surface (condition). Therefore, no hydrocarbon liquid is created at the surface, theoretically.

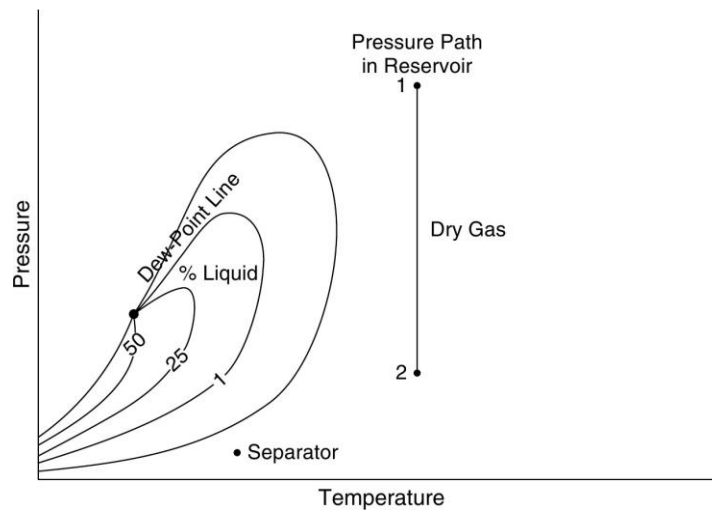


Figure 3: A typical dry gas reservoir phase diagram [reproduced from (ARNOLD, 2007)].

- Wet gas:** The majority of hydrocarbons in the reservoir and at the surface are in the gas phase. However, at the offshore processing conditions, a small fraction of the product is released as condensate (Figure 4). The term “wet gas” does not imply that the gas is wet with water, it rather refers to a hydrocarbon liquid, which can condense at the surface under certain conditions (ARNOLD, 2007). Intermediate hydrocarbons, such as propane and butane, are abundant in wet gas. Some liquids, on the other hand, tend to develop in a separation state near the surface, and this liquid is commonly referred to as condensate. The pressure route does not enter the phase envelope, as shown in Figure 4, and hence no liquid is formed in the reservoir. Separator conditions exist within the phase envelope, resulting in the formation of some hydrocarbon liquid in the separator (Bidgoli, 2020).

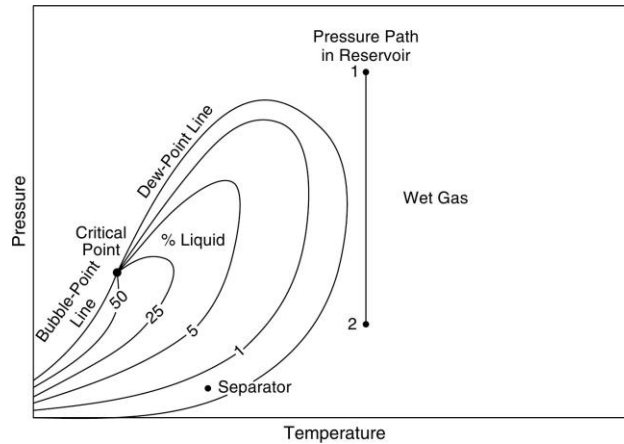


Figure 4: A typical wet gas reservoir phase diagram [reproduced from (ARNOLD, 2007)].

- Gas condensate:** The Gas Condensate reservoir, also known as a retrograde gas condensate reservoir. The condensate gas in the reservoir is completely gaseous at first (point 1 in Figure 5). Condensate Gas has a temperature and pressure higher than the fluid's critical temperature and pressure at reservoir conditions, causing it to condense into a gas (Bidgoli, 2020). The gaseous stream is usually abundant in the gaseous stream (rich gas) (NGL). Ethane, propane, butanes, and pentanes, as well as higher-molecular-weight hydrocarbons C_{6+} , are the examples of NGLs (Speight & James G, 2014). When the pressure in the reservoir drops, the fluid approaches dew point, and a large volume of liquid begins to condense in the reservoir, as shown in Figure 5 (Point 2). As the pressure drops and the depletion continues, liquid condenses form as the free liquid (Point 3).

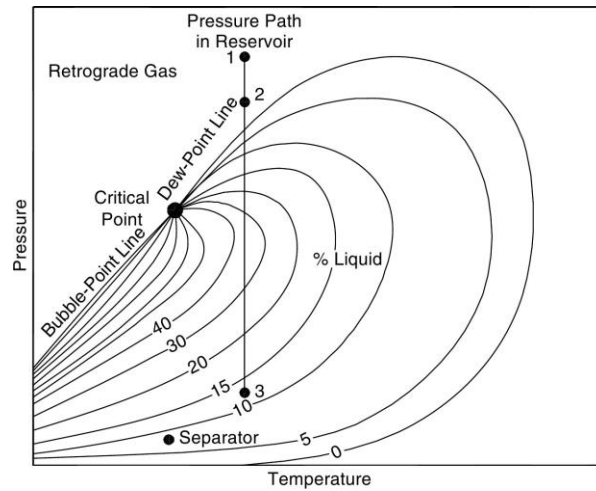


Figure 5: A phase diagram of a condensate gas reservoir [reproduced from (ARNOLD, 2007)].

- Near critical or volatile oil:** The reservoir fluid is mainly in liquid form. In comparison to Black oil reservoirs, it contains more heavy components and intermediate hydrocarbons. With the exception that the reservoir temperature of volatile oil is lower than its mixture critical temperature, which indicates that when the pressure is reduced below the bubble point, volatile oil might flash to a higher gas content.

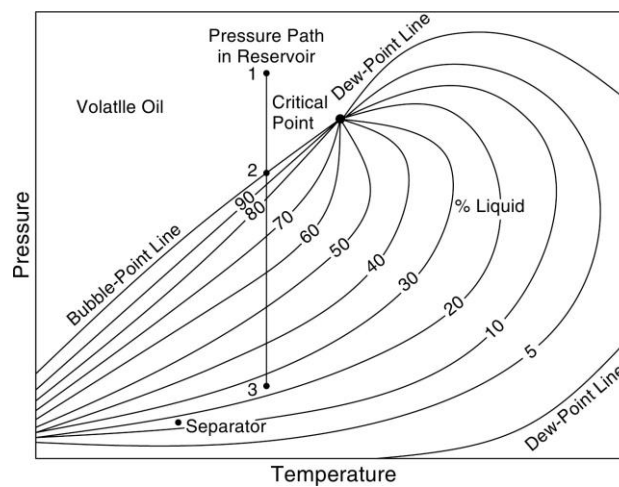


Figure 6: A phase diagram of a volatile oil reservoir [reproduced from (ARNOLD, 2007)].

- Black oil:** Hydrocarbons that are mostly large, heavy, and non-volatile. When the reservoir pressure drops along line 1→2, the oil becomes undersaturated, and if there is more gas available, it dissolves it. As the pressure decreases, the bubble point pressure branch is always reached, resulting in the development of a gas phase. At point 2, the oil has the highest concentration of dissolved gas (Figure 7). Separator conditions occur well within the phase envelope, implying that a significant volume of liquid reaches the surface (Point 3). The laboratory determined that the composition of heptane plus will be greater than 30% mole percent, indicating that black oils include a significant number of heavy hydrocarbons (ARNOLD, 2007, Bidgoli, 2020).

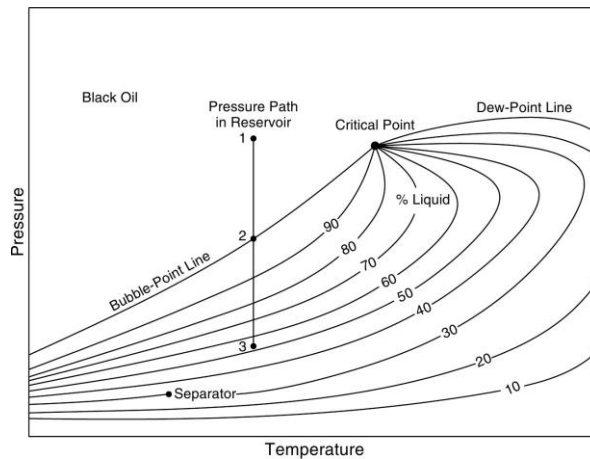


Figure 7: A black oil reservoir phase diagram [reproduced from (ARNOLD, 2007)].

However, due to the large number of distinct hydrocarbons that composing reservoir mixtures performing a full compositional analysis of those fluids is nearly impossible. Methane (CH_4), ethane (C_2H_6), and propane (C_3H_8), which are referred to as C_1 , C_2 , and C_3 correspondingly, are the lightest hydrocarbons contained in the reservoir fluid. The number of carbon atoms is used to refer to heavier hydrocarbons in the same way. The hydrocarbon in crude oil compounds is classified into one of the subclasses listed below.

- Alkanes or paraffins which are saturated hydrocarbons having the general formula (C_nH_{2n+2}) are known as alkanes or paraffins. They can be straight-chain or branched-chain components, with the latter being more valuable than the former due to the manufacturing of high-octane

gasoline. Generally, Iso – paraffins have at least one side chain, whereas normal – paraffins are straight – chain compounds.

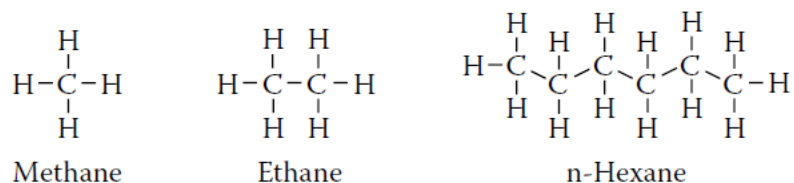


Figure 8: Example of Chemical Structures of Paraffins or alkanes (Pedersen & Christensen, 2007).

- Cyclopentane (C_5H_{10}) and cyclohexane (C_6H_{12}) are known as cycloalkanes or cycloparaffins (naphthenes) (Bidgoli, 2020). Naphthenic rings of 5, 6, or 7 carbons are commonly found in petroleum reservoir fluids (Andreasen et al., 2018). In the creation of aromatic compounds, the presence of high numbers of these cyclic compounds in the naphtha range is significant (Bidgoli, 2020).

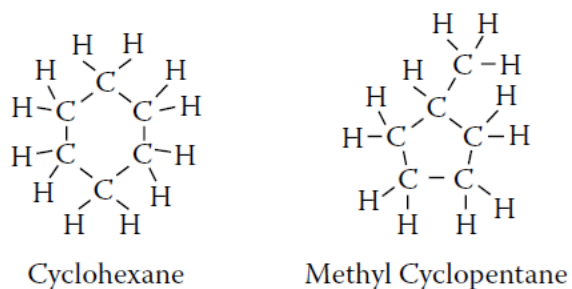


Figure 9: Example of Chemical Structures of Naphthenes (Pedersen & Christensen, 2007).

- Aromatic hydrocarbons with only one monomolecular component in the range of C_6 – C_8 have become commercially important (Bidgoli, 2020). The most basic aromatic molecule is benzene (C_6H_6), however polycyclic aromatics like naphthalene are abundant in reservoir fluids ($C_{10}H_8$) (Pasquale, 2007).

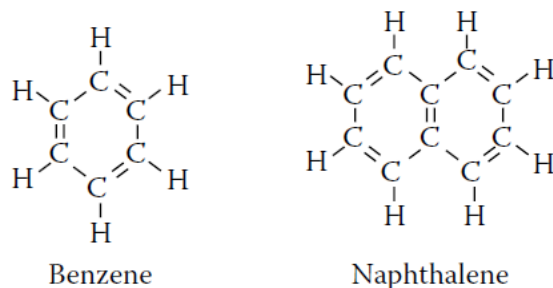


Figure 10: Example of Chemical Structures of Aromatics (Pedersen & Christensen, 2007).

2.2. Physical properties of petroleum reservoir fluids

Furthermore, based on the data in Table 1 for the physical qualities of several reservoir fluids constituents, physical properties of reservoir fluids components can vary greatly.

Table 1: Physical Properties of Petroleum Reservoir Fluid Components (Hu, 2017).

Component name	Chemical formula	Molecular weight (g/mol)	Boiling point (°C)	Density at 20°C	Critical temperature (°C)	Critical pressure (bar)	Acentric factor
Nitrogen	N_2	28.02	-195.8	0.0012	-147	33.9	0.04
Carbon Dioxide	CO_2	44.01	-78.5	0.0019	31.1	73.8	0.225
Methane	CH_4	16.04	-161.6	0.0007	-82.6	46	0.008
Ethane	C_2H_6	30.07	-87.6	0.0028	32.3	48.8	0.098
Propane	C_3H_8	44.09	-42.1	0.002	96.7	42.5	0.152
n-Hexane	C_6H_{14}	86.17	68.8	0.659	234.3	29.7	0.296
Cyclohexane	C_6H_{12}	84.16	80.7	0.779	280.3	40.7	0.212
Benzene	C_6H_6	78.11	80.1	0.885	289	48.9	0.212
n-Decane	$C_{10}H_{22}$	142.28	174.2	0.730	344.9	21.2	0.489
Naphthalene	$C_{10}H_8$	128.17	218	0.971	475.3	40.5	0.302

Generally, different gases have varied physical properties (density, boiling point, molecular weight, and so on) even at the same temperature and pressure. However, it has been discovered

that near the critical point, almost all gases exhibit extremely similar characteristics (Hu, 2017). A reliable characterization of petroleum reservoir fluids can be classified into grouping hydrocarbons heavier than nC_5 according to carbon number fractions based on their normal boiling points.

Compositional analysis is performed on a reservoir sample, which can be obtained from the bottom of the well (single phase) or after a first separation following extraction (gas and liquid sample). After flashing both types of samples at standard pressure and temperature conditions (1.01 bar, 15°C), the two phases are separated and analysed individually. For the characterization of reservoir fluid samples, analytical techniques such as gas chromatography (GC) and true boiling point (TBP) are commonly utilized.

The most frequent approach for determining the proportions of the heavier C_{7+} components in a petroleum mixture is gas chromatography (GC) (Bilal Younus, 2021). (TBP) analysis according to ASTM D-2892 provides physical narrow fractions which can then be investigated for molecular weights, densities, viscosities, and other properties. The molecular weight is determined by studying the freezing point depression phenomena in the presence of a suitable solvent. Density, on the other hand, is normally assessed by the average of densitometers (Pasquale, 2007). In general, well pressures typically range from 150 bar to 410 bar, with temperatures rarely exceeding 100°C whereas, water and absorbed gases are present in the liquid phase to be removed under these conditions (Society of Petroleum Engineers, s.d.). Operating pressure and temperature of well fluids are lower than in the reservoir after extraction, and the flow is a mixture of oil, gas, and water. Hence, a separation procedure is needed to divide the flow into the various phases for subsequent processing (Pasquale, 2007).

2.3. Vapor pressure measurements

In the offshore process the gas condensate specification is necessary to minimize hydrocarbon emissions during the storage and transport of condensate, which is based on vapor pressure measurements (Speight & James G, 2014, Jasper et al., 2019).

Table 2: The standards used to produce this gas condensate specification are listed in the table below.

ASTM D2879-18 (ASTM, 2018)	Isoteniscope is a standard test method for determining the vapor pressure-temperature relationship and the first decomposition temperature of liquids.
ASTM D323-15a (ASTM, 2015)	Standard Test Method for Vapor Pressure of Petroleum Products by Reid Method
ASTM D6377-16 (ASTM, 2016)	Standard test method for determining the vapor pressure of crude oil by VPCR _x (Expansion Method)

I. True vapor pressure

The TVP can be measured directly with an isoteniscope, as described in ASTM standard D2879-18 (ASTM, 2018). The approach works with crude oil with a TVP of 0.133 kPa to 101.3 kPa at the specified temperature. The mixture must not have a vapor pressure more than 0.133 kPa at 50°C in order to apply this procedure. The pressure due to the vapor of the sample is balanced against a known pressure of an inert gas in this procedure. There should be no air present because the TVP measurement requires a liquid sample. It must be eliminated from the sample prior to the measurement if it is present. As a result, it is inconvenient for field or laboratory measurements that necessitate the use of operating personnel (Mokhatab et al., 2015, Jasper et al., 2019).

II. Reid vapor pressure

Unlike TVP, RVP measurements can carry air. It is defined as the absolute vapor pressure exerted by a substance at 100°F (37.8°C) and is a measure of the volatility of the Crude Oil produced. RVP is an experimental measure that follows the ASTM D – 323 standard test technique. RVP values for Crude Oil are typically between 0.69 and 0.83 bar (10 – 12 psi). Standard D323-15a by ASTM is a method for measuring the RVP of a liquid that is applicable to volatile crude oil (ASTM, 2015). The chilled sample is filled into the liquid chamber of the vapor pressure apparatus, which is connected to the vapor chamber, which has been heated to 37.8 °C in a bath. The assembled apparatus is immersed in a bath of 37.8 °C until it reaches a constant pressure. In general, the RVP is the rate of change of pressure.

Chapter 3: Offshore oil and gas production

The aim of this chapter is to introduce the usual offshore facilities to present the different steps from the raw reservoir fluids to the finished products. Main specifications are related to these steps are also introduced in this chapter. The main goal is to provide an overview of the oil and gas production consisting of their separation process in offshore platforms.

3. Offshore oil and gas facilities

The main goal of an offshore oil and gas processing plant's is to transport and separate oil, gas, and water extracted from a set of underground reservoirs. Gas is compressed for re-injection, gas lift, and/or export, and oil is transported in pipes or stored in cargo tanks for export to separate crude oil from the gas (Jasper et al., 2019). After additional processing, LNG, and other products such as propane and butane are produced pipes transmit the streams from the several wells and clusters to a production manifold via a seabed network (Pasquale, 2007). The production manifold can send the stream to the first stage of a production separator train, which separates oil, gas, and water (either to a test separator or to the first stage of a production separator train) (Jasper et al., 2019). Reservoir fluids are nowadays extracted from wells up to 3000m – 3500m below the seabed, accounting for 30% of global Crude Oil production and 27% of global Natural Gas output (Total S.A., 2015). In the next section, offshore facilities based on size and depth of the seabed will be discussed.

The primary design of an offshore plant depends on first, the oceanic circumstances, such as site temperature, and second, well conditions, such as well composition, usable years of operation, distance from cost, and depth from sea level. ETA-OFFSHORE-SEMINARS (1976) says that the composition of the crude oil has a big impact on the primary and utility systems of an offshore plant. One of the most common offshore structures is the following:



Figure 11: Shallow water complex offshore platform (aau student, Csanyi, 2017)

Figure 11 illustrates shallow water complex platform are distinguished by their numerous independent platforms that are connected by gangway bridges to various processes and services, which typically found in water depth up to 100 meters (Speight & James G, 2014).

A typical offshore platform consists of several main plants where processes such as separation, compression, treatment, and pumping are carried out, and utility plants are taken into consideration to provide the necessary power and heating for the main plants, according to (ARNOLD & STEWART, 1998) with the title of design of oil handling systems and facilities. (ARNOLD & STEWART, 1998) also stated that, a number of important factors, including well-fluid flow rates, operational pressures and temperatures, well fluid characteristics, and how productions are handled in the end, might affect a processing plant's performance.

BP et al; 2004, indicated that the separation train is the most crucial component for oil and production in the third phase of Azari, Chirag, and Gunashli after finishing the full Field Development of the petroleum platform's main plants. However, BP et al; 2004, did not specified the details of the used crude oil composition and operating pressure of sequential separators, but the report contains some important information. According to the result from the optimized case of the report, reduction of fuel consumption is achieved by lowering the operating temperature in the second stage of the separation train and raising the operating pressure in the third stage of the separation train.

3.1. Separation of Reservoir fluids

The goal of separating reservoir fluids from underwater wells is to generate a Gas stream that is as free of C_{3+} hydrocarbons as feasible, as well as Crude Oil that is stable in storage conditions. Indeed, the Crude Oil generated must not vaporize when delivered into the storage tank and in the event of minor variations in storage pressure and/or temperature.

As shown in Figure 12, these goals are frequently achieved by gradually lowering the fluid's pressure and temperature through a multistage separation consisting of two or three separators, which is referred to as a separation train. The initial separator is normally a vessel where Crude Oil, gas, and water are separated primarily at different conditions of pressure and temperature. The gas phase rises to the top of the vessel and is sent to the gas treatment unit, where it is processed for dehydration, C_{3+} condensate removal, and other purposes. The water from the treated reservoir fluid goes to the bottom of the separator and is then routed to the produced water treatment unit, before being reinjected into the well or disposed of in the sea. Crude oil passes from the first separator to the second separator, which reduces pressure and/or temperature. The evaporation of the light hydrocarbons remaining present in the liquid phase releases a little additional fraction of gas in this way. A little amount of water from oil and gas wells is removed from the liquid (forms with the oil, or injection water) and then is combined with the water coming out of the first separator. A third separator may be necessary for a final separation to meet the liquid product's stability and recovery criteria, as well as to reduce water content. Gas from the second and, finally, the third separators is compressed and blended with gas from the first separator. The crude oil is then kept in tanks before being transported to an oil treatment unit to remove any remaining water and salts, and ultimately to a refinery plant (Pasquale, 2007).

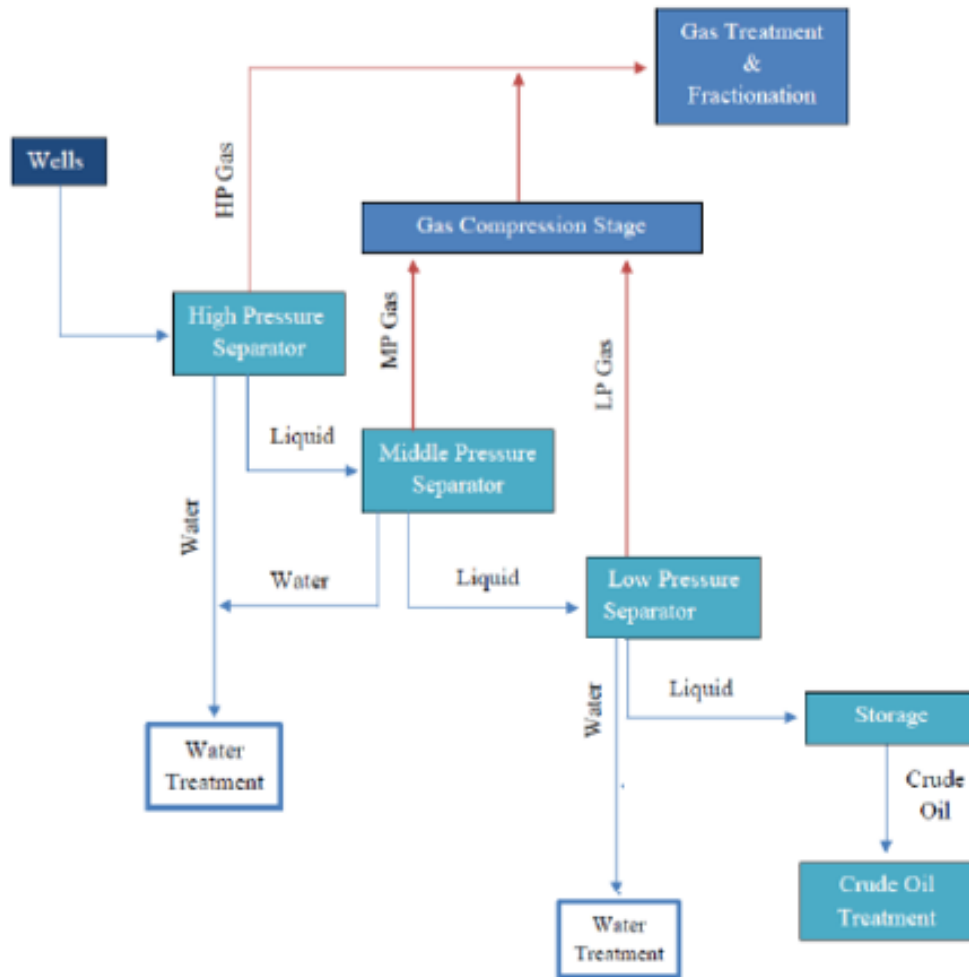


Figure 12: Oil and gas separation train [reproduced from (Pasquale, 2007)].

Separators are categorized mostly according to the number of phases they can handle. According to this idea, two types of separators are extensively employed in the oil and gas industry (Pasquale, 2007).

- **Two Phase Separator:** It divides the reservoir fluid flow into two phases: oil and gas.
- **Three Phase Separator:** It uses density to separate the well fluid into oil, gas, and water flows.

Moreover, separators can also be classified into two different categories based on their configurations (Pasquale, 2007):

- **Horizontal Separator:** This is a popular choice for three-phase separations and reservoir fluids with a low gas-to-oil ratio (Gas-to-Oil Ratio, or GOR). It's simple to set up and provides enough residence time for the liquid–liquid split, as well as a large liquid phase area that decreases turbulence.
- **Vertical Separator:** It is an excellent choice for high-GOR reservoir fluids and two-phase separations. The removal of deposits is easy in this separator.

3.1.1. Crude oil treatment

Crude oil still includes up to 2% water, as well as soluble and insoluble salts, after it has been separated. Additional treatments are needed to eliminate those salts and water traces, as they are likely to create a more stable emulsion and sediments over time, causing corrosion, incrustation, and bubbles in the pipeline during oil transmission.

In addition, any oil-in-water emulsion must be disrupted before final oil-in-water separation (Sutherland, 2012). Onshore facilities generally perform crude oil dehydration by infusing the appropriate amount of a demulsifier chemical and introducing the oil into an electrostatic coalescer. This method of dehydration is the most popular since it reduces the amount of space and weight necessary for the operating equipment, as well as the amount and cost of the demulsifier to be employed. After separation and treatment, the physical qualities and several compositional elements of crude oil can vary greatly.

3.1.2. Gas treatment

Gas stream produced by the separation train make up by the methane, ethane, and traces of higher hydrocarbons. Moreover, water vapor, carbon dioxide, hydrogen sulphide, nitrogen, and other contaminants are also present in minor amounts. Generally, gas treatment is the process of removing acid gases such as CO_2 and H_2S . This is required to meet their requirements and maintain the equipment's integrity (avoiding corrosion and plugging problems) (Jaspart et al., 2019). The initial step is the removal of hydrocarbons heavier than methane and ethane, as well as acid gases.

The former involves chilling the gas below its dew point and then passing the resulting gas–liquid mixture through a high-pressure three-phase separator to separate water, gas, and liquid hydrocarbons (Pasquale, 2007). CO_2 is vented or used as an injection fluid in enhanced oil recovery operations once it is extracted from the gas. Venting CO_2 can only be released into the atmosphere if environmental restrictions allow it (Kidnay, 2011, Jaspert et al., 2019).

Afterwards the gas stream is then dehydrated using glycols, a pressure swing absorber, or membranes. Mercury is removed using molecular sieves and nitrogen traces are rejected using cryogenic distillation, resulting in a high-concentration nitrogen gas stream. The produced water treatment unit receives the water removed by the condensate removal and dehydration, while the hydrocarbon condensate is transported to the oil refinery (Kim et al., 2014).

3.1.3. Water treatment

The water recovered from the separation train and gas processing restrains Traces of oil and other impurities. The produced water stream can be reused by reinjecting it into the reservoir to increase gas production, must be able to flow through the rock's small passageways (Pasquale, 2007). This means it will have to be filtered free of fine solids, possibly down to $2\mu\text{m}$ at the point of injection (though oil will not have to be separated from it as thoroughly) (Sutherland, 2012). The oil concentration, in particular, must be reduced to less than 40 mg/L. The sand cyclone is the first step, which removes sand impurities, which are then washed again before being discharged. The water stream is then passed through a hydro-cyclone to remove oil droplets: a steady vortex forces the separation of the oil phase in the centre from the water on the side. The recovered oil phase is typically recycled to the separation train's third separator. A degassing drum is used as the final treatment step to further remove oil droplets from water: gas dispersed in the water stream begins to rise to the surface, dragging oil droplets with it. As a result, the produced oil film is drained, and water can be discharged into the sea (DEVOLD et al., 2006).

3.2. Summary

The literature review showed that there are different types of offshore installations operation and discussed about the brief of Gas, crude oil, and water treatment. The key operating parameters for the performance of desired productions are operating pressures and temperatures of the separation process, heaters, compressors, and pumps. These operating parameters are crucial to understand their effects on separators, which are placed well inside the two-phase region of the separators. This simplifies the problem of forming phase equilibrium calculation to vapor-liquid equilibrium calculation. Therefore, in the next chapter, the theoretical foundations of thermodynamic modelling will be discussed.

Chapter 4: Thermodynamic modelling

Exploration and production in offshore platforms often require working on under difficult and harsh circumstances. In this regard, phase behaviour modelling of the separators in oil-gas separation platforms is very important from an economical and environmental point of view. Phase equilibrium calculations form the basis of a numerous applications, such as compositional reservoir simulation, wellbore, and separation processes (Gaganis & Varotsis, 2014). In fluid thermodynamics modelling, these calculations are used when there are large compositional effects in the system, which allows a more realistic and reliable description of component transfer between phases (Qiu et al., 2014). This chapter is structured in terms of the most widely used and efficient thermodynamic methods used in the oil and gas system in distinct pressure and temperature to model the separator.

4. Thermodynamic Analysis

The use and application of thermodynamics of petroleum fluids in the oil and gas industry ranging from production and refining of crude oil and gas to processing of petrochemicals. According to the First Law of Thermodynamics, energy cannot be created or destroyed, but can only be transformed from one form to another. An energy analysis thus indicates changes from one form of energy to another and enables the tracing of energy flows within a given system. In steady-state conditions and steady-flow processes, the energy balance for a control volume is written as:

$$\dot{Q} - \dot{W} = \sum \dot{m}_{out} h_{out} - \sum \dot{m}_{in} h_{in} \quad \text{Eq.1.}$$

where \dot{Q} and \dot{W} are the heat rate and power, respectively, m is the material stream's mass flow rate, and h is the specific enthalpy. The most important thermophysical properties required in petroleum refining for process and equipment design are enthalpy and vapor liquid equilibrium (fugacities) (Qiu et al., 2014). The information provided by enthalpies and fugacities is sufficient

to compute the mass and energy balances across the most unit operations in a refinery. Flash calculations and multiphase equilibrium algorithm used to determine the phase behaviour, compositions and properties of oil and gas system at distinct PT conditions. Perhaps, aspen HYSYS is capable of carrying out the isothermal two-phase PT-flash calculations using the compositions of well-fluid. Thermodynamic modelling of oil and gas, in equilibrium was based on the VLE algorithm which will be discussed in the in 4.1.3 section.

4.1. Flash Calculations

Flash calculations problems assume that the feed stream comprises with the global composition represented for a set of molar fractions (z_i), comprises one mol of chemical species that do not react. Therefore, equation 2 and 3 respectively provides global and component balance equations for two phases in equilibrium, L = Liquid phase, V = Vapor phase.

$$L + V = 1 \quad \text{Eq. 2}$$

$$Lx_i + Vy_i = z_i \quad \text{Eq. 3}$$

In equation 2 and 3, L is the moles number of liquid with molar fraction x_i ; V is the moles number of vapor, with molar fraction y_i . These equations can be combined shown in equation 4:

$$Vy_i + (1 - V)x_i = z_i; \quad i = 1, N_c \quad \text{Eq. 4}$$

Substituting the definition of equilibrium ratio ($K_i = y_i/x_i$) and solving x_i and y_i using equation 5, results in:

$$x_i = \frac{z_i}{1 - V + VK_i} \quad \text{Eq. 5}$$

$$y_i = \frac{K_i z_i}{1 - V + VK_i} \quad \text{Eq. 6}$$

Where, y_i is the mole fraction in vapour phase, and x_i is the mole fraction of liquid phase for component i . Generally, the “K-value” K_i depends on temperature T, pressure P, and composition

(both x_i and y_i). Basically, in flash calculations each component of a mixture of hydrocarbons will be in equilibrium at a particular pressure and temperature. Therefore, the amount of vapor depends on the overall composition of the fluid because the mole fraction of any one component in the gas phase depends on every other component in that phase (Becker et al., 2015)(see figure below).

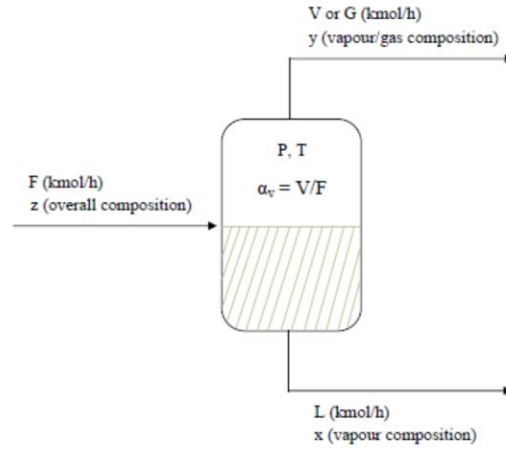


Figure 13: Flash tank (Becker et al., 2015).

Flash calculations are applied for processes involving vapor/liquid equilibrium (VLE). From the figure 13 we can see that, a typical process that requires flash calculations, is the process of separating a feed stream (F) into a vapor (V) and liquid (L) product. In general, flash calculations are simple operations that combine the VLE- equations with the component mass balances and, occasionally, the energy balance. If K_i for each component and the ratio of total moles of vapor to total moles of liquid (V/L) are known, then the moles of the component i in vapor phase y_i and the moles in the liquid phase x_i can be calculated. The value of V obtained from equation 5 and 6 can be calculated by the solution of the non-linear Rachford-Rice equation (Rachford & Rice, 1952).

$$f(V) = \sum_{i=1}^{N_c} (y_i - x_i) = \sum_{i=1}^{N_c} \frac{z_i(K_i-1)}{1-V+VK_i} = 0 \quad \text{Eq. 7}$$

In general, the simplest flash is usually to specify p and T (pT -flash), because K_i mainly depends on p and T . Thus, to find out V/L we may need to solve Rachford-Rice equation. Newton-

Raphson method with 10^{-6} tolerance, as shown in Figure 14 below, was applied to solve the Equation 7. Moreover, negative flash concept also implemented in this step.

4.1.1. The Cubic Equation of state

Using cubic EOS, such as the Soave-Redlich-Kwong, 1972 and Peng-Robinson, 1978 equations, is used to estimate thermodynamic properties for both liquid and vapor phase. Thus, the compressibility factor of the phases as well as the fugacity for each component in each phase of the mixture were calculated. Equation of state models have proven to be very reliable in predicting properties of most hydrocarbon-based fluids under a wide variety of operating conditions. In each case, they are presented as follows (Soave, 1972; Peng robinson 1976): In Equation 8 and 12 has presented the Peng Robinson EOS.

$$p = \frac{RT}{V-b} - \frac{a\alpha(T)}{V(V+b)} \quad \text{Eq.8.}$$

$$a = \frac{0.457235R^2T_c^2}{p_c} \alpha(T) \quad \text{Eq.9.}$$

$$b = 0.07780 \frac{RT_c}{p_c} \quad \text{Eq.10.}$$

$$p = \frac{RT}{V-b} - \frac{a(T)}{V(V+b)b(V-b)} \quad \text{Eq.11.}$$

After doing some algebraic operations and thermodynamic concept applications, Equation 8 and 11 can be rewritten in their cubic form which is relating to phase compressibility factor (Z) (Ahmed. T, 2007).

$$Z^3 - Z^2 + (A - B - B^2)Z - AB = 0 \quad \text{Eq.12.}$$

$$Z^3 - (1 - B)Z^2 - (A - 2B - 3B^2)Z - (AB - B^2 - B^3) = 0 \quad \text{Eq.13.}$$

Where A and B parameters are presented as:

$$A = \frac{a_m p}{(RT)^2} \quad \text{Eq.14.}$$

$$B = \frac{b_m p}{(RT)} \quad \text{Eq.15.}$$

The term a_m and b_m for each equation can be found in [26]. The equation 14 and 15 demonstrate respectively, the expression for fugacity obtained using SRK and PR EOS with Van der Waals classical mixing rules (Ahmed. T, 2007).

$$\ln \frac{\tilde{f}_i}{p} = \frac{\bar{b}_i}{b} (Z - 1) - \ln(Z - B) + \frac{A}{B} \left[\frac{\bar{a}_i}{a} - \frac{\bar{b}_i}{b} + 1 \right] \ln \left\{ \frac{Z}{Z+B} \right\} \quad \text{Eq.16.}$$

$$\ln \frac{\tilde{f}_i}{p} = \frac{\bar{b}_i}{b} (Z - 1) - \ln(Z - B) + \frac{A}{B} \frac{1}{2\sqrt{2}} \left[\frac{\bar{a}_i}{a} - \frac{\bar{b}_i}{b} + 1 \right] \ln \left\{ \frac{Z+(1-\sqrt{2})B}{Z+(1+\sqrt{2})B} \right\} \quad \text{Eq.17.}$$

4.1.2. VLE (Vapour-liquid Equilibrium) Algorithm

A vapor liquid equilibrium flowchart that depicts the computation procedure in two loops shown in figure below. To carry out the flash calculations, Rachford-Rice equations was solved within the internal loop. As PR EOS gives more robust flash calculations to determine oil and gas phase equilibrium, in the external loop, the PR EOS and VLE convergence were used to calculate the Z factor and fugacity.

The PR EOS is the modification of the Redlich Kwong (RK) Equation of state that corresponds to a lower compressibility factor of about 0.307, therefore presenting the VLE of natural gas and oil separation system accurately (Neto & Bannwart, 2015).

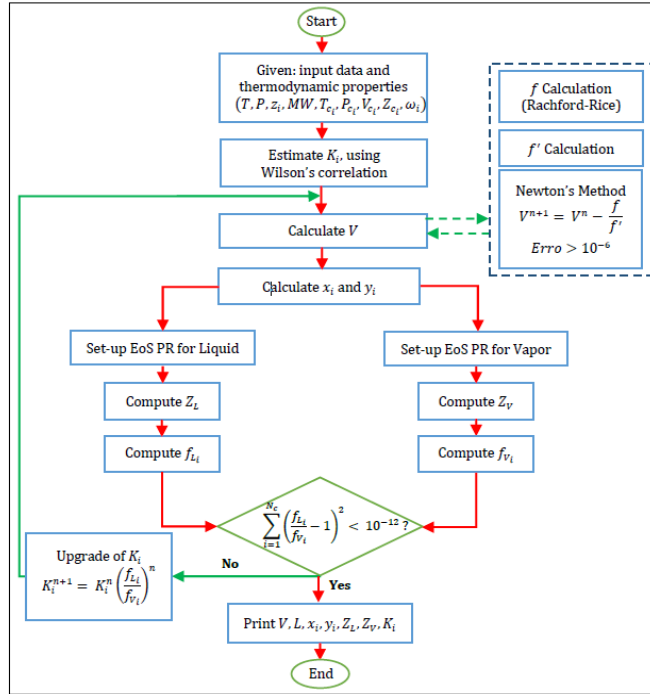


Figure 14: VLE algorithm flowchart using isothermal two-phase flash calculations and the PR-EOS (Neto & Bannwart, 2015).

4.2. Summary

In order to evaluate the performance of the algorithm implemented in the figure above, simulations at a large range of pressure and temperature were performed in Aspen HYSYS. The isothermal two-phase PT-flash shows a compatible solution with the commercial thermodynamic packages in Aspen HYSYS for the well fluid. From a thermodynamic point of view, compared to PR EOS, SRK EOS and other cubic EOS calculates the liquid molar volume which is significantly less accurate than the gas molar volume. Consequently, PR EOS is the latest development among all other cubic EOS, which gives the more accurate value of state variable calculation (P, V, T) and reasonable for liquid as well as non-polar gases. The function is well suited for the vapor pressure data of hydrocarbon and does fairly well for these materials. Therefore, the thermodynamic commercial package could be used in Aspen HYSYS to separate the well fluid into a liquid and vapour phase through the two-phase PT-flash and VLE calculations for an efficient oil and gas production in offshore plant.

Chapter 5: Problem formulation

Offshore platforms are complex structures that are used to extract subsea oil and gas deposits. They cost billions of dollars or euros to build. These funds are awarded based on cost-effective projects that are designed on a case-by-case basis for specific petroleum wells. In the previous section an overview of the offshore platform structures has been discussed where we found that, optimizing both new and existing offshore oil and gas facilities to maximize profit is a crucial goal for the oil & gas Industry in the near future. Indeed, because a single platform can receive fluids from different wells, and those streams can vary their operating conditions, compositions, and flow rates, where the operating conditions of the units on old facilities may be adjusted in response to changes in the feed stream conditions to be treated. On the other hand, it is economical to construct new offshore platforms with the goal of maximizing the amount of oil and gas produced and through optimization process allowing the adjustment to adapt operating parameters in response to changes in feed composition and operating conditions to meet the optimization aims (For example, maximum profit).

The aim of this study is to maximize the production of gas and the oil in a separation train design using an objective function and statistical data treatment to find out the optimum operating point for maximum profit value. First, Aspen HYSYS was used as the process simulator for rigorous modelling and simulation of oil and gas production processes. The process model includes an oil separation, gas condensation, and gas recompression train to reflect the interactions of all the equipment and to depict a more accurate outcome considering the profit value calculated by the oil and gas sales through the formulated objective function. Second, develop optimization algorithms to determine the best operating pressures and temperatures for separation trains by applying Response surface methodology (RSM), where the optimization subsequently performed on the formulated response surface.

In order to accomplish the necessary aims, investigating which operating parameters is the most efficient at maximizing oil and gas production that will help to detect the utmost profit value

out of the oil and gas sales in separation train process, the resulting problem statement is the following question.

Which operating conditions affects the most in maximizing oil and gas production that helps to find out the maximize profit value?

The question is answered by determining the effects of different operating conditions by developing a flowsheet in a commercial software called Aspen HYSYS as process simulator to study the separation process using a sequence of three stage separators, where pressure and temperature are gradually reduced. The separation of well fluids in this study includes separating the well fluid into a liquid and vapour phase using two-phase separators, where the separators will be modelled using a powerful thermodynamic package Peng Robinson EOS built in Aspen HYSYS by PT-flash calculations for an efficient oil and gas production in the process. The separation aims to maximise the recovery of intermediate components (C_3 , C_4 , C_5) in the oil while maintaining its stability. The optimizations of the oil and gas production thus involves the investigation of the optimal operating pressures and temperatures of the separators for the maximum profit value through Response surface methodology (RSM).

Based on the project formulation, the main focus of the study is the following:

1. Design a Simulation train design flowsheet using Aspen HYSYS to study and simulate well fluids by different operating parameters.
2. Determine the impact of processing parameters on the recovery of intermediate hydrocarbons and energy consumption.
3. Build the statistical treatment to evaluate the predicted values of profit.
4. Using predicted values of profit conduct Response Surface Methodology (RSM).

Chapter 6: Methodology

The description of the implemented mathematical modelling and methodologies used in the current study is presented in this chapter.

6. Experimental plan

To meet the objective of this study, process design configurations are to be carried out using Aspen HYSYS. The result should be to determine the optimum operating conditions to maximise the profit of oil and gas sales. The experimental set up is divided into three main tasks consisting of the background information on process description, energy consumption, statistical analysis, and optimization procedure. Finally proposing a statistical method and optimization technique to find out the desired result. This approach taken to satisfy each of the tasks is presented in the following subsections.

The experimental plan is shown in figure 15 below.

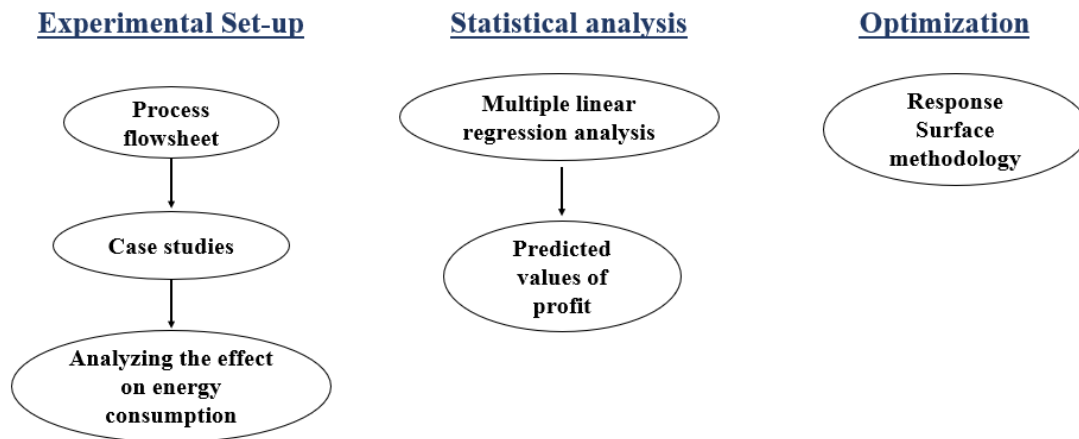


Figure 15: Experimental plan.

Since offshore gas-processing system designs vary from field to field and depend on the composition of the produced streams, only conceptual material was gathered from the literature,

upon which the simulation of the process design was built and fitted into the case study involved. Then analysing the case studies on oil and gas production system and energy consumption. To achieve the desired separation, adjusting pressure and temperature is the general strategy to separate well fluids into the two phases of oil and gas. To do that, nine different operating conditions are to be selected on the performance of first stage separator. For each of that operating conditions nine different operating parameter are to be chosen for the performance 2nd stage separator. In total 81 simulation run are to be conducted, which called as the full-factorial design of experiments. In next step, statistical analysis is to be performed using those 81 different operating parameters to find out the predicted values of objective function (Profit). On the performance of statistical analysis optimum operating conditions are to be find out based on the 1st stage and 2nd stage separator pressure and temperature using a robust optimization technique Response surface methodology (RSM). In this technique, the main goal is to meet the optimum parameter to design the separation process that maximizes the amount of oil and gas produced to increase the income of oil ang gas sales.

6.1. Process Description

A schematic process flow sheet forming a typical offshore oil and gas simulation train for the studies presented in Figure 16. The separation train is consisting of three stages named as S1, S2 and S3, coupled with gas recompression operating at different pressures and temperatures (to meet the maximum profit). All separator modelled as two-phase separator within only liquid and vapor phase, whereas in reality they are 3 phases (oil, gas and water) but water is disregarded. Each stage begins with *PT*-flash calculations followed by the separation of gas and oil. The feed is regarded as being water-free because the goal of this work is on optimal separation of oil and gas. The separation train is a multistage process that gradually depressurizes the feed mixture while simultaneously separating the gas and liquid phases. To regulate the temperature of these separator is provided by heat exchangers upstream in each separation stage. The saturated gas exiting from each separator is cooled down, which could lead to condensation. The condensates are separated from the gas in compressors (Compressor 1, compressor 2) and recycled back into the separation train at the stage $i+1$, except for the last stage to enhance the separation performance between light and intermediate hydrocarbons. In addition, a compressor is usually used to raise the pressure of

this discharged upstream before connecting with the gas stream that comes from another separator. In addition, to improve the effectiveness of the separation between light and intermediate hydrocarbons, an offshore oil production platform also contains a vapor condensation train that recycles the condensate back into the crude oil, which are SD2, SD3 in this case. The process configuration is elaborated in the following sections.

The well fluid is routed through the first stage separator, S1, in which oil and gas is separated. Overhead gas and oil are the two product streams from the 1st stage separator. Hence, the gas is collected from the top of the vessel, while the oil collected from the bottom of the column. The oil exiting a separator is further depressurized and fed to the following downstream separator with the exception of the oil exiting the 3rd stage separator of the train, which is exported or sent to the storage tank. Thus, oil is routed through via a pressure control valve, Valve 2, and cooler, E2, to the 2nd stage separator, S2, operated at a lower pressure, where oil and gas is separated. The oil input is then transported via, Valve 2, and cooler, E3 and directed to the third (final) stage separator.

The separated oil comes out as the oil export stream. The discharged upstream from the third stage separator is cooled down through E4, before it goes to the knock-out drum, SD3. Then the gas compressed a bit in compressor 2 at 3rd stage pressure and mix back into the 3rd stage separator, S3, while the 3rd stage separator works by reducing the pressure and temperature at atmospheric conditions. The vapor compressed up to 2nd stage separator from where the 2nd vapor coming at 2nd stage pressure. Note that, due to cooling and subsequent partial condensation, there may also exist additional liquid condensate streams in the compression system. Thus, the stream condensed a bit in Mixer, M3 and comes out at 2nd stage pressure then cool down in E5 and routed to the knockout drum, SD2. From SD2 the vapor phase is knocked out to be fed into the compressor 1 at 2nd stage pressure, and the discharged liquid out is mixed into the Mixer, M1, which comes out as Mix 1 out to mix back into the 2nd stage separator. On the other hand, the compressed vapor 2 is then then further mixed with the vapor that is discharged from the inlet separator into the Mixer,

M4, where SET-1 is used to compress the 1st vapor up to the export gas pressure. Then, finally the gas exits the facilities as the export gas stream, which is reasonable for this process.

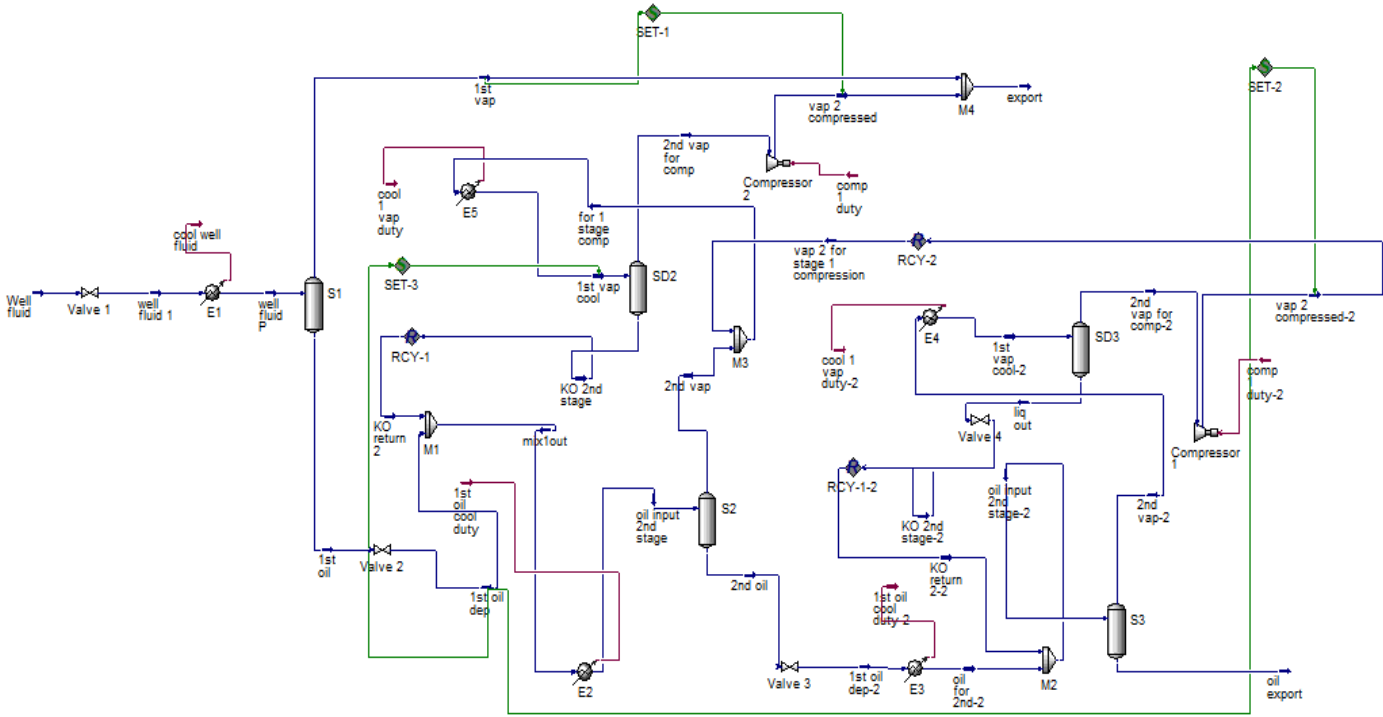


Figure 16: A schematic process flow sheet of an offshore oil and gas simulation train.

6.1.1. Fluid Description

The reservoir fluid investigated in this work was adapted from Willersrud et al., 2013 and composition and fluid characterization of the fluid are presented in Table 3. The components up to C_5 are real single components (alkanes), such as, methane, ethane, propane, i-butane, n-butane, i-pentane, and n-pentane, whereas the components from C_6 to C_{19} are pseudo components representing hydrocarbon fractions of specific carbon atoms.

The critical parameters (critical pressure, critical temperature, critical volume, and acentric factors) for defined components were estimated internally by Aspen HYSYS. Figure 16 illustrates

the fluid's phase envelope. It shows the bubble point and dew points of the well fluid at different pressures. The cricondentherm is 283.54°C and the cricondenbar is 234.3 bar.

Table 3: The composition and characterization for the investigated well-fluid.

Component	Chemical formula	Mole fraction
Nitrogen	N_2	0.0067
Carbon-di-oxide	CO_2	0.0064
Methane	CH_4	0.5633
Ethane	C_2H_6	0.0763
Propane	C_3H_8	0.0482
i-butane	C_4H_{10}	0.0074
n-Butane	C_4H_{10}	0.0135
i-Pentane	C_5H_{12}	0.0046
n-Pentane	C_5H_{12}	0.0048
n-Hexane	C_6H_{14}	0.0054
n-Heptane	C_7H_{16}	0.0071
n-Octane	C_8H_{18}	0.0073
n-Nonane	C_9H_{20}	0.0037
n-Decane	$C_{10}H_{22}$	0.2366
Undecane	$C_{11}H_{24}$	0.0014
Dodecane	$C_{12}H_{26}$	0.0011
Tridecane	$C_{13}H_{28}$	0.0011
Tetradecane	$C_{14}H_{28}$	0.0009
Pentadecane	$C_{15}H_{32}$	0.0008
Hexadecane	$C_{16}H_{34}$	0.0005
Heptadecane	$C_{17}H_{36}$	0.0007
Octadecane	$C_{18}H_{38}$	0.0004
Nonadecane	$C_{19}H_{40}$	0.0003
Icosane	$C_{20}H_{42}$	0.0015

6.1.2. Simulation setup

The process flow diagram shown in Figure 16 above is modelled in the process simulation flow sheet. The simulation software package solves Peng-Robinson equation of state individually to calculate the *PT*-flash at each unit. The study was conducted for well fluid as feed stream and the feed flow rate was set at 343.1 kgm/h. At the inlet the well stream with a temperature of 40°C and a pressure of 50 bar enters a two – phase separator (1st stage separator) with a gas outlet from the top and a liquid hydrocarbon outlet from the bottom. The parameters that were manipulated were the temperature and pressure of the well stream at 1st stage and 2nd stage separator. The parameter values were set based on the following criteria: The first stage separator, S1, pressure and temperature were assumed at wellhead pressure and temperature to reduce compression cost. The third stage separator, S3, pressure and temperature were set to 1 bar and 25°C (at atmospheric conditions) and the second stage separator, S2, pressure and temperature was set as intermediate in order to have an equal pressure ratio between 1st to 2nd stage and 2nd to 3rd stage. More particularly, is that the pressure in each separator must be lower than in the previous separator.

Table 4: Operating conditions and design parameters of the flowsheet.

Parameter	Design (range) at 1st stage Separator	Design (range) at 2nd stage separator	Design (range) at 3rd stage separator
Temperature (°C)	60 to 50	45 to 30	25
Pressure (bar)	50 to 25	24 to 12	1
Feed flow rate (kgmol/h)	343.1	-	

However, the operating pressure of the 3rd stage responsible for exporting oil to the oil storage. The operating conditions, and design parameter in ranges of the flowsheet diagram can be found in Table 4. Since pressure and temperature of the first separator is varying from 50 bar to 25 bar and 60°C to 50°C. It might be noticed that small changes occur in the flow rate of oil and gas until reaching nearly atmospheric pressure and temperature in the third stage. The pressures

and temperature of the separation train (P1 & T1, P2 & T2, P3 & T3) was taken as design variables. The design parameter applied to the variables in the present study based on the existing offshore facilities and practical considerations (assuming North Sea conditions).

Typically, the choice of process parameter influences the proportion of gas and liquid entering the separator. The 1st stage separator operating condition was operated at nine different conditions such as: High pressure and high temperature (HP, HT: 50 bar, 60°C), High pressure and intermediate Temperature (HP, IT: 50 bar, 55°C), High pressure and low temperature (HP, LT: 25 bar, 50°C), Low pressure and intermediate temperature (LP, IT: 25 bar, 55°C) etc. Combining the nine different conditions of first stage separator carrying nine possible different pressure and temperature combinations of second stage which resulted in 81 simulation runs. Thus, there are 81 design variables regarding selecting optimal operating conditions, to do calculation of profit values.

Before conducting any process optimization (i.e., the parameters are related by an objective function that describes the interaction between the variables), dependent and independent variables must be defined. The primary purpose of optimization is to maximize the profit.

6.2. Objective function

The optimization objective can be expressed in a variety of ways. The goal can be to increase oil/gas production (Ghaedi et al., 2014, Bahadori et al., 2008, Ling et al., 2013), reduce power consumption, maximize profit. The objective of the optimization in this case is profit maximization as shown in Equation 18 and 19. The profit calculation is done by subtracting the operating expenses of the fuel consumption from total produced gas and is expressed in USD per day. In the equation below, the profit from oil sales based on the calculated oil flow rate/export oil, using the prices 71.384 \$/barrel oil and a value of 4.3938 \$/MMBtu taken from on 30th December 2021.

The objective function is therefore set as follows:

$$\varphi = \varphi_{oil} + \varphi_{Sales\ gas} \quad \text{Eq.18.}$$

$$\varphi = \$_{oil} * Q_{oil} + \$_{gas} * F_{Sales} * HHV \quad \text{Eq.19.}$$

Where, φ is the profit function and φ_{oil} is the profit from oil sale is based on the volumetric flow rate of oil Q_{oil} ($\frac{\text{barrel}}{\text{day}}$) using oil price of $\$_{oil} = \$71.384/\text{barrel}$. The profit from gas sales $\varphi_{Sales\ gas}$, is calculated using a value of $\$_{gas} = \$4.384/\text{MMBtu}$, where the revenue loss associated subtracting the required fuel gas consumption for power generation from the total produced export gas, before calculating $F_{sales\ gas}$ (kg/h).

$F_{sales\ gas}$ is the sales gas mass flow rate.

All power needs were required to be met internally by a fraction of the exported gas, which is, $P = \eta \cdot HHV \cdot F_{Fuel}$, used as fuel gas, where P is the power requirement and F_{Fuel} is the mass flow rate of the fuel gas required internal energy needs, $\eta = 0.30$ is the turbine efficiency. HHV (kJ/kg) is the higher heating value if gas produced because we assumed that we have condensation that will recover some of the latent heat of vaporization per unit of fuel burned then we can use the higher heating value. The sales gas required for fuel gas is subtracted from the total gas production yielding the export gas rate is given by,

$$F_{sales\ gas}(\text{kg/h}) = F_{total\ produced\ gas}(\text{kg/h}) - F_{Fuel}(\text{kg/h}) \quad \text{Eq.20.}$$

$$\text{Where, } F_{Fuel} = \frac{E(\text{kJ/h})}{\eta * HHV(\text{kJ/kg})} \quad \text{Eq.21.}$$

After that to calculate the $\varphi_{Sales\ gas}$ the mass flow rate $F_{sales\ gas}$ was multiplied by Higher heating value (HHV), in which HHV was converted to MMBTU/kg using the conversion factor $1\text{kJ} = 9.4782\text{E-}7\text{ MMBTU}$.

$$\varphi_{Sales\ gas} = F_{sales\ gas}(\text{Kg/h}) * HHV(\text{MMBTU/kg}) * \$_{gas}(\$/\text{MMBTU}) \quad \text{Eq.22.}$$

Other utilities, such as manufacturing chemicals, are assumed to be unaffected by process parameters changes. Labour, maintenance, indirect charges, and other costs are not included in this analysis since they are less susceptible to changes in variables than the direct cost of power generation. Oil and gas prices are volatile, and they may exhibit opposite price trends in the short term, while they appear to correlate over on a longer time periods.

Furthermore, the profit for the chosen fluid is heavily influenced by the oil sales price hence it might be considered that the findings obtained using the aforesaid objective function will be generally applicable and mostly unaffected to oil and gas price fluctuations.

In addition, the optimization of a complicated process simulation model is frequently non-linear, necessitating either derivative-free approaches or the estimation of numerical derivatives for optimization. However, depending on the model's complexity and the number of variables, the latter may result in excessively time-consuming objective function evaluations (Andreasen, 2020). Therefore, we performed regression analysis.

6.3. Energy consumption

Each unit that requires energy is investigated. Basically, we can see huge effect by the changes of process parameter. All power requirements of each simulation set up were calculated to be covered internally by a fraction of the exported gas:

$$P = \eta \cdot \text{HHV} \cdot F_{\text{Fuel}} \quad \text{Eq.23.}$$

Where P is the power requirements has already mentioned in the previous section. The total energy consumption (E) in the process is the sum of energy consumed by the compressors 1 and 2 in this study. The amount of condensation taken place in the gas compression system can have a huge impact on the power requirements for compression. The adiabatic efficiency of all compressors was set at 0.75 in terms of gas compression.

$$E = E_{C1} + E_{C2} \quad \text{Eq.24.}$$

Where E_{C1} and E_{C2} are the 1st stage and 2nd stage compressor energy respectively. F_{Fuel} is the mass flow rate of gas required for internal energy needs. The fuel gas flow of related streams was automatically modified $\eta = 30\%$, the turbine efficiency, in order to represent revenue loss due to reduced gas export flow rate, which results in a more attractive setup in terms of energy efficiency.

After each compression stage, the gas stream is cooled down before moving on the next compression stage, which resembles the isothermal compression process to a certain extent and reduces the overall amount of power required to achieve the desired end pressure. Compressors energy consumption rises if the pressure ration or flow increases. Concerning the cooler, the energy demand is higher if the flow rises and if the temperature difference between the inlet and the outlet of the cooler is increased. The gas compression systems are generally the processes that requires the highest cooling demands, as the associated gas needs to be cooled after each compression operation from 100 to 150°C to 30 – 50°C. Crude oil may also be cooled for further export. However, the separation module is the system that requires the highest heating demand, in order ensure that the hydrocarbon fractions are properly separated between the liquid and gas phases. The fuel gas required for power generation may be preheated before being processed into the gas turbines.

The aim is to calculate F_{Fuel} (Mass flow rate of fuel gas), that is the minimum energy requirements for compression, corresponding to the maximum gas production. Then subtract it from the total produced gas to evaluate the sales gas flow rate, $F_{Sales\ gas}$.

6.4. Optimization

As we already discussed about the effect of T1 & P1 and T2 & P2 as high, intermediate, and low on profit per kilograms, to find the optimal solution the very first step we needed to do is to find the objective function. This is vital. In this work by modelling the process simulation with all the involved unit operation, the optimization can be begun by changing the relevant settings of process parameters (temperature and pressure levels) in each stage (Andreasen et al., 2018). It has long been of scientific and practical interest to optimize surface facilities for the separation of reservoir fluids into separate liquid and gaseous phases. The ultimate objective is to find out the maximum profit using the profit function, where we wanted to find which combination of 1st stage and 2nd stage temperature and pressure would give the maximum profit to offshore oil and gas plant. There are a variety of ways to do the optimization. (Ghaedi et al., 2014a) used a genetic algorithm with a commercial process simulator to maximize the crude oil production in a flour stage separation train for both a crude oil and a gas condensate well stream. It was found that oil

production might be raised by about 2% and 8%, for crude and gas condensate, respectively, by optimizing the pressure in the first three separators (Bahadori et al., 2008). (Kylling, 2009) used brute-force optimization to optimize a two-stage separation train and three different feed composition compatible with a North Sea platform, and (Bahadori et al., 2008) used a stochastic optimization approach to optimize 3- and 4-stage separation trains while also considering the constraint of oil stability at stock tank conditions (Maschietti, 2019). (Andreasen et al., 2018) applied response surface methodology (RSM) and used the process simulation to perform virtual or surrogate experiments. The overall performance process is optimized in terms of power consumption within the constraints of quality specifications for oil and gas export, respectively, by conducting surrogate experiments in accordance with the Design of experiment (DoE) and building multiple linear regression for the formulated response surface(s). In this study, the optimization is done by finding out the optimal solution we performed multiple linear regressions and later used the RSM (Response Surface Methodology) to find the optimum operating parameter using the predicted profit values.

6.5. Experimental design and statistical analysis

Response surface methodology is a collection of statistical and mathematical approach in which the response of interest is affected by a number of independent variables and the goal is to optimize the response. The experimental plan may be a 2 or 4-level or more level of full factorial experiments with a few or many independent variable or factors that allows for the estimation of both main effects and all interaction between variables. As the number of variable increases, the number of required experiments for full factorial experimental plan grows exponentially. In this case, the effect of independent variable P1, T1, P2, T2 on Profit was investigated to find the level of 1st stage and 2nd stage pressure and temperature that maximizes the profit of the offshore oil and gas sales. There are two types of Response Surface Modelling: a) Central composite Design (CCD), b) Box-Behnken Design (BBD) (Statistics, 2016).

In this work, the experimental data were designed using a Central Composite Rotatable Design. The RSM was applied to the experimental data using a commercial statistical tool Rstudio. As a central composite design can efficiently estimate first and second order polynomial terms.

Typically, CCD can model a response variable with curvature by adding centre and axial points to a previously/done factorial design (detail will be discussed in the next section). In addition, central composite design is especially useful in sequential experiments to often build on previous factorial experiments (in this case simulation data) by adding axial and centre points. However, Box-Behnken Design (BBD) do not have an embedded factorial design, they are not suited for sequential experiments. For this reason, to conduct the study Central composite design (CCD) was used.

6.5.1 Experimental design using Central Composite design

The most popular class of designs used to determine the number of experiments to be evaluated for the optimization of the variables and responses is the central composite design, or CCD, originally developed by (Box G. E. P. ; Wilson, 1992) and improved by (Statistics, 2016). In general, the CCD includes a 2^k factorial with its origin at the centre points n_c , $2k$ axial or star runs fixed axially at a distance, say α , and from the centre to create the quadratic terms and replicate experiments at the centre, where k is the number of variables. The minimum, intermediate, and maximum values of each variable are labelled as -1, 0, and +1, respectively.

Basically, the practical deployment of a CCD model leads through a sequential experimentation, where at first, a 2^k factorial design is to be created to fit a first-order model. If this model has shown a lack of fit and the axial runs are then added to enable the inclusion of the quadratic terms in the model. The CCD is a very effective design for fitting the second order model.

There are two requirements in the CCD model that must be specified; one is the distance α of the axial points from the design centre, and the number of centre points n_c . The axial points are chosen in a way that allows for rotatability α to ensure that the variance of the model prediction is constant at all points equidistant from all the design centres (Box G. E. P. ; Wilson, 1992). Typically, four to six centre points are recommended based on number of factors. This is illustrated in Table 14 in Appendix 1. The distance α , should ensure that a second order response surface design to be rotatable.

In this study we used a face-centred central composite design (CCD). As we were working with P1, T1, P2, T2, therefore for four variables, the recommended number of experiments at the centre is six to calculate the repeatability of the of the method (Douglas C. Montgomery, 2008). The response function (Y) would be Profit. Thus, the total number of experiments required for the four independent variables is $2^4 + (2 * 4) + 4 = 28$, Figure 1 shows the required CCD model and the co-ordinates for $k = 4$ factors.

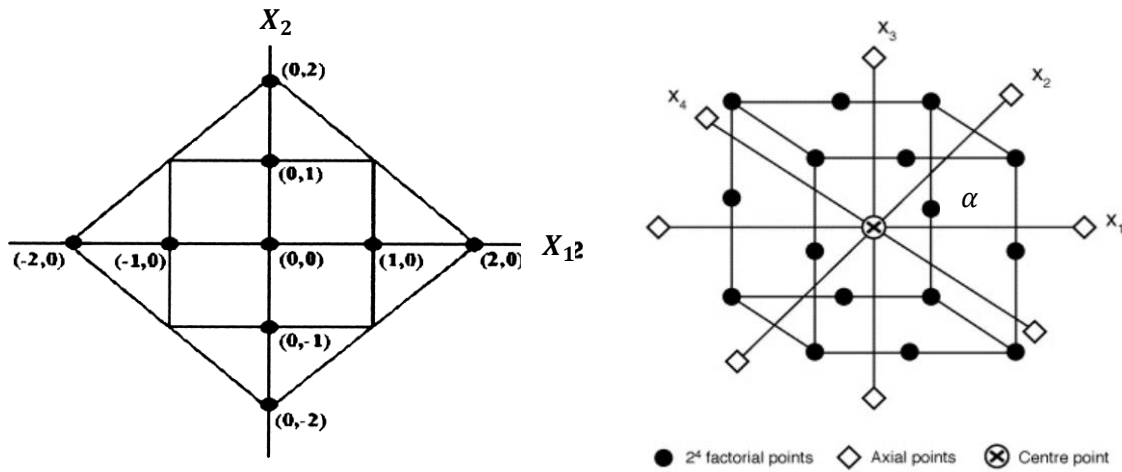


Figure 17: CCD model for four factors or variables X_1, X_2, X_3 and X_4 (Douglas C. Montgomery, 2008).

Hence, the design procedure of response surface methodology is as follows:

- 1) Creating a sequence of experiments for educate and reliable measurements of the desired response according to central composite design (CCD).
- 2) Emerging a mathematical second order response surface model for the dependent variable, y , of interest (referred to as response variable) as a function of independent variables, X_j .
- 3) Check for lack-of-fit (normal residuals, random residuals, outliers etc.)
- 4) Finding the optimal set of experimental settings to yield a maximum or minimum value of response.
- 5) Using two- and three-dimensional plots to illustrate the direct and indirect effects of process parameters. In the contour plot, lines of constant response were drawn in the X_1, X_2, X_3, X_4 plane. Each contour associates to a particular height of the response surface.

The response surface is expressed as follows,

$$y = f(X_1, X_2, X_3, X_4)$$

The main goal is to optimize the response variable y . It is presumptive that the independent variables are continuous and subject to minor experimental error. It is necessary to find a suitable approximation for the real functional relationship between independent variables and the response surface. Usually, a second-order polynomial is utilized in response surface methodology. Hence, for screening first order response surface model was used shown in Equation 25,

$$y = \beta_0 + \beta_1 X_1 + \beta_2 X_2 + \beta_3 X_3 + \beta_4 X_4 \quad \text{Eq.25.}$$

Where y is the response variable and $\beta_1, \beta_2, \beta_3, \beta_4$ are the regression coefficient of X_1, X_2, X_3, X_4 respectively. Then, for optimization, second order response surface model was used with k factors expressed in equation below.

$$y = \beta_0 + \sum_{i=1}^k \beta_i X_i + \sum_{i=1}^k \beta_i X_i^2 + \sum_{i=1, i < j}^{k-1} \sum_{j=2}^k \beta_{ij} X_i X_j \quad \text{Eq. 26.}$$

$$y = \beta_0 + \beta_1 X_1 + \beta_2 X_2 + \beta_3 X_3 + \beta_4 X_4 + \beta_{11} X_1^2 + \beta_{22} X_2^2 + \beta_{33} X_3^2 + \beta_{44} X_4^2 + \beta_{12} X_1 X_2 + \beta_{13} X_1 X_3 + \beta_{14} X_1 X_4 + \beta_{23} X_2 X_3 + \beta_{24} X_2 X_4 + \beta_{34} X_3 X_4 + \varepsilon \quad \text{Eq. 27.}$$

Where, y = the measured response for each test (Profit)

For the coded variable X_1, X_2, X_3, X_4 used for expressing P1, T1, P2, T2 respectively as follows ($X_1 = P1, X_2 = T1, X_3 = P2, X_4 = T2$). Where, the coefficients of the polynomial model were interpreted by,

β_0 = constant term, which is the average value of the experimental responses,

$\beta_1, \beta_2, \beta_3$ and β_4 = is the linear effects means main effect of the coded variable,

$\beta_{11}, \beta_{22}, \beta_{33}$ and β_{44} = the quadratic effects of the coded variable,

$\beta_{12}, \beta_{13}, \beta_{14}, \beta_{23}, \beta_{24}$ and β_{34} = interaction effects of the coded variable $X_1, X_2, X_3,$ and X_4 .

The β is the coefficients should be determined in the equation. 3 above, (the second order model), are estimated by the least square method.

As different variables are generally expressed in different units and/or have different bounds of variation, their effect can only be compared if the variables are coded. Therefore, a reduced and centred variable X_i is associated with each independent variable U_i (Equation 28), in which using CCD coded variables are developed to build the model.

$$X_i = \frac{U_i - U_{io}}{\Delta U_i} \quad \text{Eq. 28.}$$

Where, X_i = centred and reduced variable (X_1, X_2, X_3, X_4)

U_i = natural (independent) variable (U_1, U_2, U_3, U_4)

U_{io} = the value of U_i at the centre of the experimental data (Equation 29):

$$U_{io} = \frac{U_{i.max} + U_{i.min}}{2} \quad \text{Eq. 29.}$$

U_{io} = maximum value of U_i (Upper limit of the natural experimental data or simulation data)

$U_{i.min}$ = minimal value of U_i

ΔU_i = centre of the experimental data (Equation 30)

$$\Delta U_i = \frac{U_{i.max} - U_{i.min}}{2} \quad \text{Eq. 30.}$$

The factor level settings for each simulation data are summarized in Table 5. The full experimental plan of the applied face-centred composite design (*Handbook of Statistical Methods*, 2012) is given in Table 14, Appendix 1.

Table 5: 2^4 factorial level used in central composite design (CCD).

Code levels (X_1, X_2, X_3, X_4)	P1, bar	T1, °C	P2, bar	T2, °C
Max. Starting point (+2)	55	65	32	52
High (+1)	50	60	24	45

Mid (0)	37.5	55	18	40
Low (-1)	25	50	12	30
Min. Starting point (-2)	15	45	6	25

The response variable (dependent variable) is collected from the table 1 for each combination of P1, T1, P2 and T2, which table is recorded after convergence of each process simulation according to the simulation experimental plan.

Least square method

Generally, the least square method expressed in matrix form shown below.

$$Y = \beta X + E \quad \text{Eq. 31.}$$

Where, Y is the matrix of measured values and X is defined to be a matrix of independent variables and E is the residual errors respectively. The eq. 4 can be solved by matrix form:

$$\beta = (X^T X)^{-1} X^T Y \quad \text{Eq. 32.}$$

The mathematical model was assessed using Multiple linear regression model (Julian J. Faraway, 2004) for the response variable. Multiple regression model helps to predict and find out the optimum outcome of the response variable depending on the condition of significance of the independent variables. 81 observations on the profit (Y) of an offshore oil and gas production sales and four process variables: 1st stage pressure and temperature (P1, T1) and 2nd stage pressure and temperature (P2, T2) are shown in Table 6. This is used to fit a multiple linear regression model to see each one of these tools explain unique variance in profit.

Table 6: Dependent and independent variable used to perform multiple linear regression model.

Dependent Variable	Independent variable
Profit mill. \$/day	P1
	T1
	P2

To find out the relations among the variables we observed the correlation matrix and also the prediction model or fitted regression model where the substantive information about each predictor variable to predict the measured or actual values of Profit function when statistically controlling for the other, which is specified by the equation below. Note that, the first order model defined in Equation 25 can be expressed as regression equation by:

$$\hat{y}_i = \beta_0 + \beta_1 X_1 + \beta_2 X_2 + \beta_k X_k + \varepsilon \quad \text{Eq.33.}$$

Where \hat{y}_i is the predicted value of profit function and the residual is $\varepsilon = y_i - \hat{y}_i$.

6.6. Summary

The objective function can lead to increase profits in a number of offshore oil and gas facilities by adjusting the pressure and temperature values of the separator. Once a response surface model which fits the experimental data to a satisfactory level has been identified for the response variable, the response surface can be investigated. This is often done visually, as previously stated above, RSM modelling was started with a linear effects, squared and interaction terms. Analysis of variance (ANOVA) in Multiple linear regression was used to identify the significant terms in the model for the response variable. Significance was investigated by obtaining the probability level that the *P*-value calculated from the data is less than 0.005. The model adequacy was checked by R^2 , adjusted R^2 , predicted R^2 . However, all the variables will be used to perform RSM to see how they affect on the response surface (profit function). By investigating the response surface, the optimum settings can be visually identified directly.

Chapter 7: Results and Discussion

Once the process simulations of the different operating conditions were generated, such as the outlet gas flow rate, oil flow rate, calculated sales gas mass flow rate, and the total power consumption of compressors was collected and compiled in a table. Finally calculated the profit function using that table, to utilize it in generating the regression model and optimization model and the outcome of this model will be investigated in this chapter.

7. Result Analysis

The study is conducted by changing the operating conditions of each feed in 1st stage separator to investigate their effect on the separation process. Hence, key process simulation outputs such as the outlet gas and oil flow rate, calculated sales gas mass flow rate, and total power consumption. A detail calculation was made by varying the separator conditions on second stage for each T1 and P1 has shown on the Table 7 below. In second stage separator for each T1 and P1, with the varying Temperature and pressure nine simulation runs was conducted, whereby the total compressor power consumption was summarized, taking both compressor duty. In addition, more importantly the main objective profit function was calculated for each specific convergence.

Table 7: The table below gathers the process parameters that are set to meet the specifications on the crude oil and gas.

1st stage		2nd stage		Mass flow rate of oil	Mass flow rate of gas	Compressor 1 & 2 duty		Total Comp.	Mass flow rate of fuel	Oil sales	Gas sales	Profit
P1, bar	T1 °C	P2, bar	T2 °C	F_{oil} , kg/h	F_{gas} (kg/h)	C1, KW	C2, KW	E, KW	F_{fuel} , (\$/day)	φ_{oil} , (\$/day)	$\varphi_{sales\ gas}$, (\$/day)	φ , (Milli. \$/day)
<i>PI & T1 at HP=50 bar & HT=60°C</i>												
50	60	24	45	13497.8	4970.2	60.2	46.2	115.5	2.68e+01	200589.0	5255	0.2058
50	60	24	40	13498.8	4970.2	60.2	48.6	108.8	2.52e+01	200517.6	5255	0.2058
50	60	24	30	13497.8	4971.2	60.2	53.3	113.8	2.64e+01	200374.9	5255	0.2056

50	60	18	45	13497.8	4971.3	60.0	41.4	101.5	2.36e+01	201160.1	5248	0.2064
50	60	18	40	13498.8	4970.2	60.0	43.5	103.6	2.41e+01	201160.1	5246	0.2064
50	60	18	30	13497.8	4971.2	60.1	48.0	108.1	2.52e+01	201017.3	5236	0.2063
50	60	12	45	13497.8	4971.2	59.8	34.8	94.7	2.20e+01	201873.9	5263	0.2071
50	60	12	40	13498.8	4970.2	59.8	36.6	96.4	2.24e+01	201873.9	5261	0.2071
50	60	12	30	13497.8	4971.2	59.8	40.3	100.2	2.32e+01	201873.9	5261	0.2071
<i>PI & TI at HP=50 bar & IT=55°C</i>												
50	55	24	45	13515.2	4953.7	61.5	47.2	108.8	2.52e+01	202159.5	5.24e+03	0.2074
50	55	24	40	13516.4	4952.6	61.5	49.7	111.2	2.58e+01	202159.5	5.24e+03	0.2074
50	55	24	30	13515.52	4953.5	61.5	54.8	116.4	2.70e+01	202159.5	5.24e+03	0.2074
50	55	18	45	13515.28	4953.7	61.4	42.3	103.7	2.40e+01	202159.5	5.24e+03	0.2074
50	55	18	40	13516.43	4952.6	61.4	44.5	105.9	2.45e+01	202159.5	5.24e+03	0.2074
50	55	18	30	13515.52	4953.5	61.4	49.2	110.6	2.56e+01	202159.5	5.24e+03	0.2074
50	55	12	45	13515.28	4953.7	61.2	35.6	96.7	2.24e+01	202159.5	5.24e+03	0.2074
50	55	12	40	13516.43	4952.6	61.1	37.4	98.6	2.28e+01	202159.5	5.24e+03	0.2074
50	55	12	30	13515.52	4953.5	61.1	41.3	102.5	2.38e+01	202159.5	5.24e+03	0.2074
<i>PI & TI at HP=50 bar & LT=50°C</i>												
50	50	24	45	13515.2	4953.7	61.5	47.2	108.8	2.58e+01	202373.6	5.23e+03	0.2076
50	50	24	40	13516.4	4952.6	61.5	49.7	111.2	2.76e+01	202373.6	5.22e+03	0.2076
50	50	24	30	13515.5	4953.5	61.5	54.8	116.4	2.46e+01	202373.6	5.23e+03	0.2076
50	50	18	45	13516.2	4953.7	61.4	42.3	103.7	2.51e+01	202445.0	5.23e+03	0.2077
50	50	18	40	13515.4	4952.6	61.4	44.5	105.9	2.62e+01	202373.6	5.23e+03	0.2076
50	50	18	30	13515.5	4953.5	61.4	49.1	110.6	2.29e+01	202445.0	5.23e+03	0.2077
50	50	12	45	13515.2	4953.7	61.1	35.6	96.7	2.34e+01	202445.0	5.23e+03	0.2077
50	50	12	40	13516.4	4952.6	61.1	37.4	98.6	2.43e+01	202445.0	5.23e+03	0.2077
50	50	12	30	13515.5	4953.5	61.2	41.3	102.5	2.43e+01	202373.6	5.23e+03	0.2076
<i>PI & TI at IP=37.5 bar & HT=60°C</i>												
37.5	60	24	45	13485.9	4983.0	34.5	44.6	79.2	1.84e+01	201659.8	4.96e+03	0.2069
37.5	60	24	40	13485.3	4983.7	34.5	46.6	81.2	1.88e+01	201588.4	4.96e+03	0.2068
37.5	60	24	30	13481.8	4987.1	34.6	50.8	85.5	1.98e+01	201517	4.97e+03	0.2068
37.5	60	18	45	13485.9	4983.0	34.5	40.0	74.5	1.73e+01	201659.8	4.97e+03	0.2069

37.5	60	18	40	13485.3	4987.2	34.5	41.7	48.5	1.13e+01	201588.4	4.97e+03	0.2069
37.5	60	18	30	13481.8	4987.1	34.5	45.5	80.1	1.86e+01	201517.0	4.97e+03	0.2068
37.5	60	12	45	13485.9	4983.1	34.4	33.6	68.0	1.58e+01	201659.8	4.97e+03	0.2069
37.5	60	12	40	13485.3	4983.7	34.4	35.1	69.5	1.61e+01	201588.4	4.97e+03	0.2069
37.5	60	12	30	13481.8	4987.1	34.4	38.2	72.7	1.69e+01	201517.0	4.97e+03	0.2068
PI & TI at IP=37.5 bar & IT=55°C												
37.5	55	24	45	13506.8	4962.1	35.4	45.8	81.3	1.89e+01	201945.3	5.26e+03	0.2072
37.5	55	24	40	13506.2	4962.8	35.4	47.9	83.4	1.93e+01	201945.3	5.26e+03	0.2072
37.5	55	24	30	13502.7	4966.3	35.5	52.3	87.9	2.04e+01	201873.9	5.26e+03	0.2071
37.5	55	18	45	13506.8	4962.1	35.4	41.1	76.5	1.77e+01	201945.3	5.26e+03	0.2072
37.5	55	18	40	13506.2	4962.8	35.4	42.9	78.3	1.82e+01	201945.3	5.26e+03	0.2072
37.5	55	18	30	13502.7	4966.3	35.4	46.8	82.3	1.91e+01	201873.9	5.26e+03	0.2071
37.5	55	12	45	13506.8	4962.1	35.2	34.5	69.8	1.62e+01	201873.9	5.26e+03	0.2071
37.5	55	12	40	13506.2	4962.8	35.3	36.1	71.4	1.66e+01	201945.3	5.26e+03	0.2072
37.5	55	12	30	13502.7	4966.3	35.3	39.4	74.7	1.73e+01	201873.9	5.26e+03	0.2071
PI & TI at IP=37.5 bar & LT=50°C												
37.5	50	24	45	13526.5	4942.4	36.4	47.1	83.5	1.93e+01	222302.2	5.25e+03	0.2076
37.5	50	24	40	13525.4	4943.7	36.4	49.3	85.7	1.98e+01	222302.3	5.25e+03	0.2076
37.5	50	24	30	13521.3	4947.8	36.5	53.8	90.4	2.09e+01	222302.3	5.25e+03	0.2076
37.5	50	18	45	13526.6	4942.2	36.3	42.2	78.6	1.82e+01	222302.3	5.25e+03	0.2076
37.5	50	18	40	13525.5	4943.4	36.3	44.1	80.6	1.86e+01	222302.3	5.25e+03	0.2076
37.5	50	18	30	13521.4	4947.6	36.4	48.2	84.7	1.96e+01	202230.8	5.25e+03	0.2074
37.5	50	12	45	13526.9	4941.9	36.2	35.5	71.7	1.66e+01	222302.3	5.25e+03	0.2076
37.5	50	12	40	13525.8	4947.2	36.2	37.1	76.9	1.78e+01	202230.8	5.25e+03	0.2074
37.5	50	12	30	13521.7	5023.6	36.3	40.5	54.3	1.27e+01	200874.6	5.30e+03	0.2076
PI & TI at LP=25 bar & HT=60°C												
25	60	24	45	13445.4	5025.4	13.9	40.4	55.8	1.30e+01	200874.6	5.30e+03	0.2061
25	60	24	40	13443.5	5030.5	13.9	41.9	59.1	1.38e+01	200803.2	5.31e+03	0.2061
25	60	24	30	13438.4	5023.5	13.9	41.9	50.1	1.17e+01	200874.6	5.30e+03	0.2062
25	60	18	45	13445.4	5025.4	13.8	36.1	51.4	1.20e+01	200874.6	5.30e+03	0.2061
25	60	18	40	13443.5	5030.5	13.9	37.4	54.3	1.26e+01	200803.2	5.31e+01	0.2061
25	60	18	30	13438.4	5023.5	13.9	40.2	44.2	1.03e+01	200874.6	5.30e+03	0.2062
25	60	12	45	13445.4	5025.4	13.8	30.3	45.3	1.06e+01	200874.6	5.30e+03	0.2062

25	60	12	40	13443.5	5030.5	13.8	31.4	47.7	1.11e+01	200803.2	5.31e+03	0.2061
25	60	12	30	13438.4	5030.5	13.9	33.8	47.7	1.11e+01	200803.2	5.31e+03	0.2061
<i>P1 & T1 at LP=25 bar & HT=55°C</i>												
25	55	24	45	13472.4	4996.5	14.3	41.7	56.1	1.30e+01	201374.3	5.30e+03	0.2066
25	55	24	40	113470.4	4998.6	14.3	43.3	57.7	1.34e+01	201302.8	5.30e+03	0.2066
25	55	24	30	13465.1	5003.8	14.4	46.6	61.0	1.42e+01	201231.5	5.31e+01	0.2065
25	55	18	45	13472.5	4996.5	14.3	37.3	51.7	1.20e+01	201374.3	5.30e+03	0.2066
25	55	18	40	13470.4	4998.6	14.3	38.7	53.1	1.23e+01	201302.8	5.30e+03	0.2066
25	55	18	30	13465.1	5003.8	14.4	41.7	56.1	1.30e+01	201231.5	5.31e+01	0.2065
25	55	12	45	13472.6	4996.3	14.3	31.3	45.6	1.06e+01	201374.3	5.30e+03	0.2066
25	55	12	40	13470.5	4998.5	14.3	32.5	46.8	1.09e+01	201374.3	5.30e+03	0.2066
25	55	12	30	13465.1	5003.9	14.3	35.0	49.4	1.15e+01	201374.3	5.31e+01	0.2066
<i>P1 & T1 at LP=25 bar & LT=50°C</i>												
25	50	24	45	13498.0	4970.9	14.8	43.2	49.4	1.15e+01	201731.2	5.28e+03	0.2070
25	50	24	40	13495.7	4973.2	14.8	44.8	59.7	1.38e+01	201731.2	5.28e+03	0.2070
25	50	24	30	13490.1	4978.9	14.9	48.3	63.2	1.47e+01	201659.8	5.28e+03	0.2069
25	50	18	45	13498.0	4970.9	14.8	38.6	53.4	1.24e+01	201802.6	5.27e+03	0.2070
25	50	18	40	13495.8	4973.2	14.8	40.1	54.9	1.27e+01	201731.2	5.28e+03	0.2070
25	50	18	30	13490.2	4978.8	14.8	43.2	58.1	1.35e+01	201659.8	5.28e+03	0.2069
25	50	12	45	13498.2	4970.7	14.7	32.4	47.2	1.10e+01	201802.6	5.28e+03	0.2070
25	50	12	40	13495.9	4973.0	14.7	33.7	48.5	1.12e+01	201731.2	5.28e+03	0.2070
25	50	12	30	13490.3	4853.3	14.8	36.3	51.1	1.19e+01	201659.8	5.15e+03	0.2068

7.1. Case studies

7.1.1. Effect of different operating condition on Export oil and gas molar flow rate

In the offshore oil and gas plant, there are different levels of pressure and temperature exists. This section enables to observe the influence of different level of T1 & P1 and T2 & P2 on production rate of oil and gas. The case study of the reduction of T1 in the first stage of the separation train is studied between 60°C and 50°C. As for the oil and gas is significantly influenced by T1 as can be seen from the Table 5 above. Reducing the temperature of the first stage leads to a small decrease of gas production and but increase in oil production, because initially in the 1st stage separator most of the gas has produced sent to the compressor, C2 after that reducing the

temperature in 1st stage leads to create more oil. On the other hand, at low P1 gas flow rate rises and oil production decreases. As because separator 1, does not get HT that is why on separator 1 as little amount of gas produces. So that separator 3 is always a good place to save the stream flow.

However, the temperature after the second stage is changed from 45°C. to 30°C. When T2 is reduced oil flow rate increases. Reducing the T2 decreases the amount of vapor in the well stream so decreases the vapor flow rate and produces more liquid from Separator 2. It affects the gas processing unit, where more oil is produced from the 3rd separator. Sometime the effect of T2 has no effect on oil flow rate.

The flow entering the third separator increases as the P2 decrease. Since the vapor fraction also rises, the export gas flow rate at the outlet of this separator also increases. Therefore, when P2 increases the production of gas is increased.

For instance, one example in terms of the effect of HT and HP on oil and gas flow rate has discussed below.

Effect of HT=60°C and HP=50 bar

To see the effect of T1 & P1 at high temperature (HT=60°C) and intermediate pressure (HP=50bar) on well stream, the study is done by reducing the pressure input from 24 bar to 12 bar and temperature from 45°C to 30°C at the second stage has shown in figure below.

In particular, figure 18 shows the effect of operating conditions of 1st stage separator on well stream to separate and then flowing to the second stage separator for further separation, where it operates at nine different temperature and pressure ranges for further separation. Therefore, nine simulation results obtained for P2 equal to 24, 18 and 12 bar at each T2 which is equal to 45°C, 40°C and 30°C respectively.

As can be seen from the figure 18 and 19, T1 & P1 at HT and HP, the pattern of oil and gas flow rate is changing. Oil production rate rises slightly when T2 is equal 30°C, which is equal to 13540.4 kg/h. Therefore, at the reduced 1st stage temperature leads producing less vaporization, which is as expected. Therefore, well stream operating at High temperature and high pressure at the 1st stage separator causing oil production rate to go down.

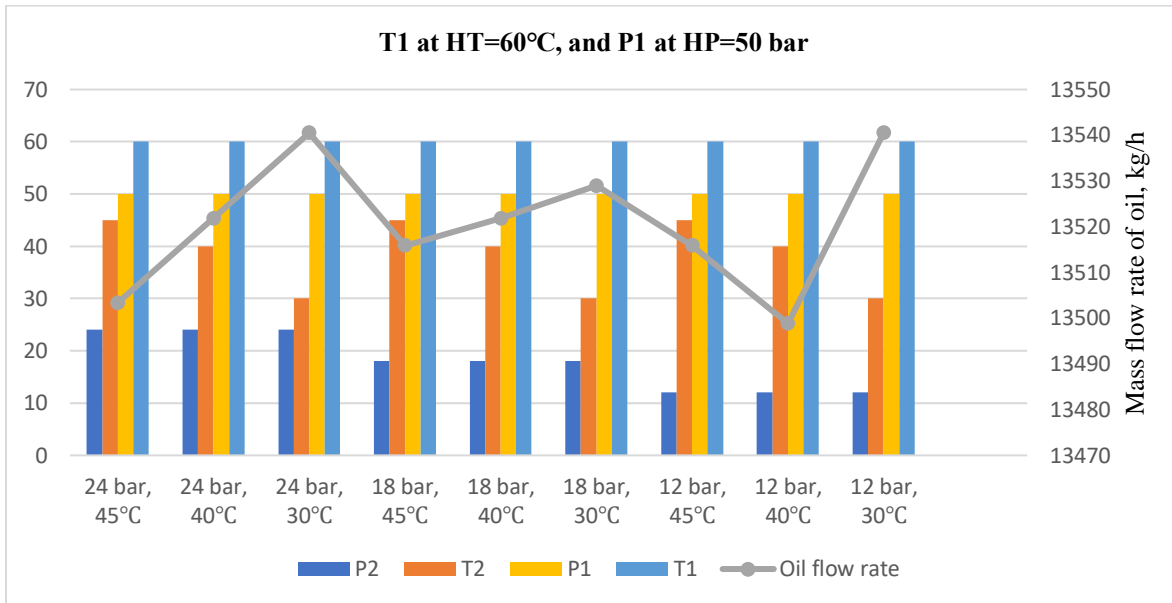


Figure 18: T1 and P1 at 60°C and 50 bar on mass flow rate of oil.

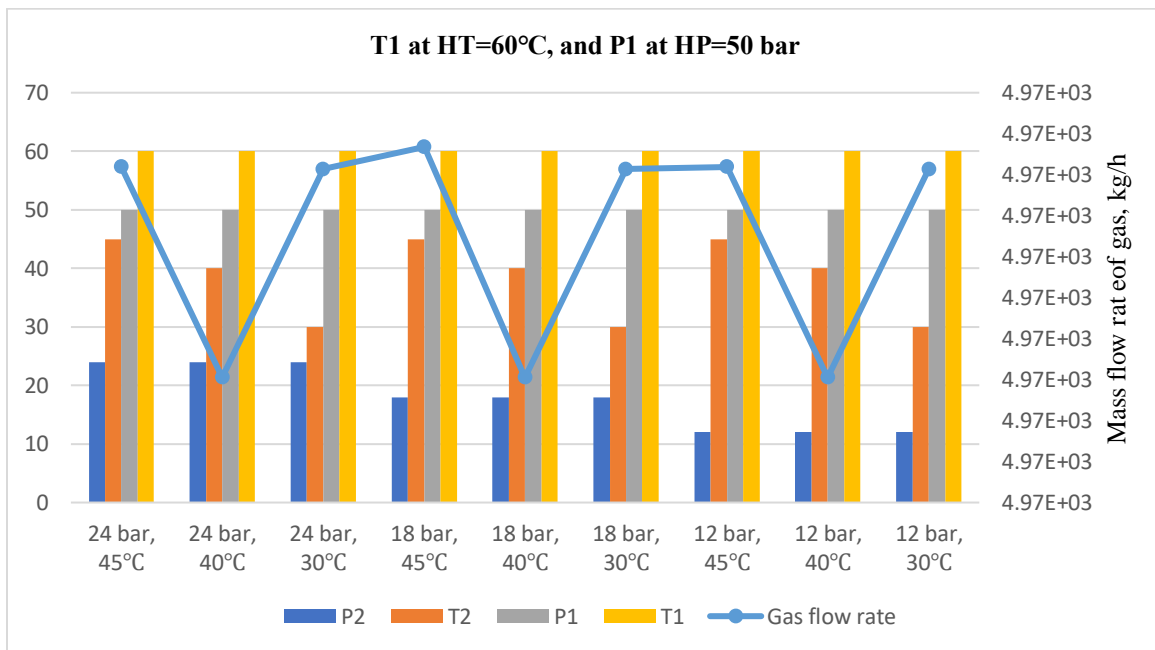


Figure 19: T1 and P1 at 60°C and 50 bar on mass flow rate of gas.

7.2. Result analysis on Energy Consumption

In previous section, oil and gas production rates according to the chosen operating variables was analysed. In this section we present results on energy consumption. We can see that the energy consumption can vary significantly. We can see from the figure gas or oil export dominate the power consumption.

Typically, the first stage separator takes out most of the gas at arrival conditions. Fuel gas is taken from the first stage separator and the residual mix of oil, gas is heated before entering the second stage separator. Note that, all the coolers in the gas processing part (E1, E2, E3, E4, E5) are modelled without any pressure drop.

7.2.1. Cooler Energy consumption

The flow through the cooler and the temperature difference between the input and outlet temperatures are the two parameters that explain the cooler energy consumption. The decrease of flow in the cooler is explained by several effects of the adjusted process parameters. When the temperature is so high the fluid in the cooler contains small amounts of liquid. Hence less flow enters the inlet separator, S1 producing less vapor and liquid. The temperature reduction of the Cooler 2 duty, E2 after the 1st stage separator, S1 produces more liquid than cooler 3, E3 (variation by 30kgmole/h). On the contrary, reducing the cooler temperature in E5, produces less amount of vapor in the stream so decrease the vapor flow rate in SD3. It affects the gas processing portion, where less liquid is sent from SD3 to the third stage of stabilization unit. The rise in the energy consumption in all coolers attached is mainly due to LP in 1st stage, it is due to the result of the increase of oil circulation in SD3.

Increasing the temperature in 1st stage increases the oil cooler duty 1, E2, as it takes more energy to cool down the oil after S1, but less to cool down the gas. In contrast, decreasing the temperature in 1st stage increases the oil cooler duty 2, E3, takes more energy to cool down the oil after S2, but less to cool down the vapor. However, decreasing the temperature in 2nd stage from 45°C to 30°C increases the cooler duty in E2 but decreases significantly in E3.

7.2.2. Compressor Energy Consumption

Compressors are responsible for 25-85% of the total energy consumption based on the operating process variable in 1st and 2nd separator. Depending on the process parameter of interest, the total energy consumption evolution is primarily driven by the compressor work (mechanical energy). The pressure reduction in 2nd stage decreases so power of the C1 and C2 increases gradually by 100 to 238KW can be seen in the figure below. The rise in the total energy consumption in compressors is mainly due to when HP in 1st stage, hence LT in 1st stage decreases the energy consumption in C1 and C2,

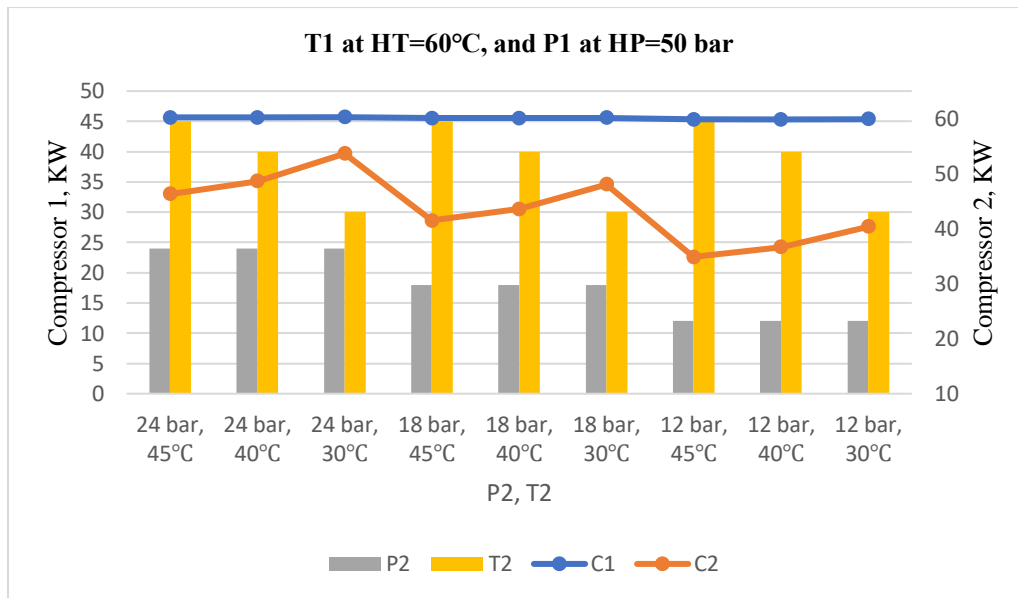


Figure 20: Energy consumption in C1 & C2 at T1=60°C and P1=50 bar.

However, the scenario is changed when due to the reduction of 1st stage pressure from 50 bar to 37.5 - 25 bar has shown in figure below. In this case, the energy consumption risen up in the C2 compared to the C1.

The choice of T1 influences mainly the compression work. The temperature reduction in the C1 produces more oil, so less vapor enters the first compressor C1 (10 -15 kgmol/h). Consequently, for T2 has no effect on C1, so does only in C2.

In the case of P2 reduction, the impact of compressors is bigger than for P1 reduction. Hence, they are responsible for 80% of the total energy consumption rise. The energy consumption in C1 is less affected by the reduction of P1 as can be seen from the simulation results but the flow increases due to vaporization. The vaporization also increases the flow rate in C2. The effect of pressure in separator 3 is less important because the pressure ratio is unchanged due to keeping it at atmospheric conditions and so on it is always good to save place for oil stabilization.

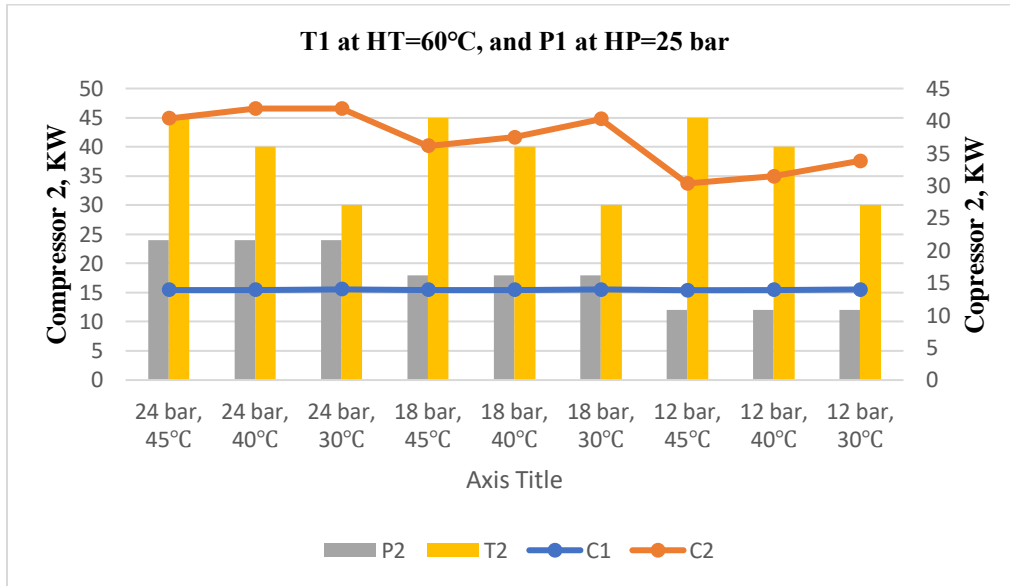


Figure 21: Energy consumption in C1 & C2 at T1=60°C and P1=50 bar.

Producing more oil and gas leads to a rise in the total energy consumption. Each unit in the process requires energy is studied. Coolers accounts for about 70% of the total energy consumption when P1 is reduced from 50 bar to 37.5 bar to 25 bar, where compressors account for only 85% of the total energy demand of the offshore oil and gas plant when P1 is at HP=50 bar.

In addition to which compressor actually affecting the most on total energy consumption, to investigate that we performed multiple regression analysis for P1, T1, P2, T2 on C1 and C2. From the result output found that, C2 is mostly responsible for the aftermost energy demand in this work. As can be seen from the table almost all the process variable has got significance level of P -value > 0.005. The model R^2 value is 0.967 and adjusted R^2 is 0.966, which is a very good model. Therefore, the P1, T1, P2, T2 can significantly predicts the C2 compressor work

Table 8: Regression model for C2 (Compressor 2).

	Estimate	Std. error	P-value	Lower 95%	Upper 95%
(Intercept)	43.0097	1.966	0.000	39.09	39.092
P1	0.24200	0.0122	0.000	0.217	0.2175
T1	-0.24623	0.0306	0.000	-0.307	-0.3072
P2	0.97526	0.0255	0.000	-0.9244	0.9244
T2	-0.36442	0.0200	0.000	-0.4043	-0.4043

7.3. Optimization result

7.3.1 Output of Regression model for Profit

Correlation matrix

In figure below (Figure 22) we can see the plot for multiple regression model, where we can see the scatter plot matrix. In the left column gives us the association between profit & T1, profit & P1, then profit & T2 and at last Profit & P2. These figure shows us the assumptions of linearity between each predictor and the outcome variable. In the very left it is the partial correlation between each one these predictors in relation to the outcome and they reveal separate correlation and scatter plot run for each bivariate association here. In the upper diagonal we can see the correlation values.

In the figure 22 we can see the correlation between T1 & P2 equals 0 or correlation between P1 & T2 is 0 and between T1 & P1 is also 0. However, correlation between profit & T2 is -0.05, negatively correlated and profit & T1 is -0.59 which is a moderate-sized correlation that reveals a negative linear correlation range between 0 to 1 positive negative and so 1 or -1 means a perfect positive or a perfect negative linear association. The correlation between profit and P1 is 0.40 but with T1 it is -0.59, which means at low T1 and high P1 profit has linear association with P1 and T1. In addition, there is no collinearity issue between variables. Therefore, from the output we can say that there is no violation of our assumption.

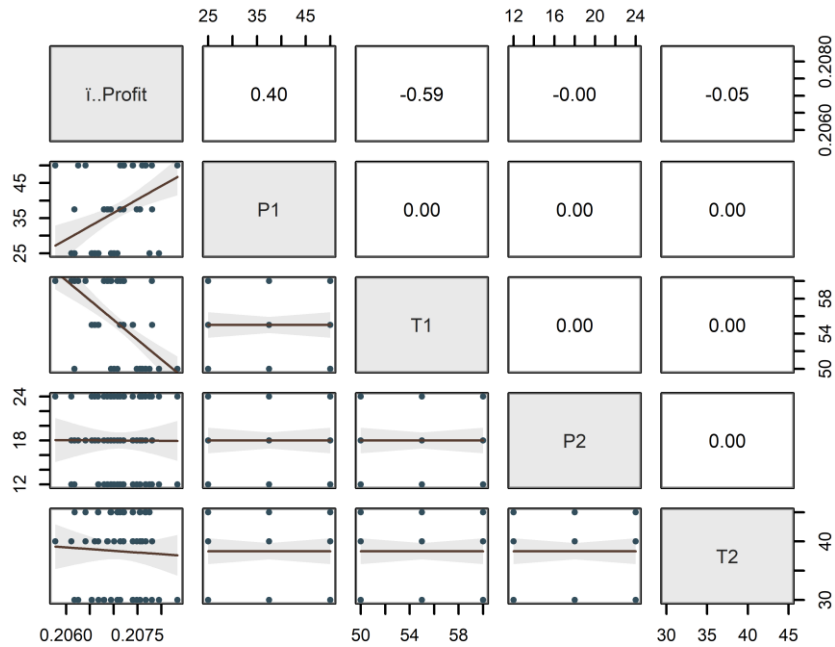


Figure 22: Correlation matrix among the variables.

Estimated model for Profit

In Table 9, we can see the substantive information about the extent with each predictor variable. The intercept value (β_0) of coefficients of profit is 0.21147691, and P -value is $0.0000 < 0.005$, which is statistically significant from 0. Now if we look at P1, the estimate (β_1) is 0.00002396, and P -value is $0.0000 < 0.005$ (which is typically the α value) and we also found out the 95% confidence as well, which is good. For T1 regression coefficient (β_2) is -0.00010429 and P -value is $0.0000 < 0.005$, this is negatively statistically associated with profit function, when controlling the other variable. That means T1 & P1 both of these variables statistically associated and explained incremental variability in profit.

However, for T2 and P2 the P -value is $0.0000 > 0.005$, which is statistically not significant, therefore these variables are removed from the regression model. Hence, the intercept value will be used to predict the future value or fitted values of Profit based on the predictor variable T1, P1. The R^2 value of the model is 0.505 and adjusted R^2 is 0.422.

Table 9: Prediction model for Multiple regression model.

	Estimate	Std. error	P-value	Lower 95%	Upper 95%
(Intercept)	0.2107105	0.0006756	0.000	0.2092648	0.2120562
P1	0.0000207	0.0000042	0.000	0.0000123	0.0000290
T1	-0.0000762	0.0000105	0.000	-0.0000971	-0.0000552
P2	-0.0000005	0.0000087	0.951	-0.0000180	0.0000169
T2	0.0000042	0.0000069	0.548	-0.0000178	0.0000096

Finally, the prediction model with the regression coefficients reported to two decimal places using Equation 33 which is, where \hat{y}_i is the predicted values of profit and $X_1 = P1$ and $X_2 = T1$.

$$\hat{y}_i = 0.2107105 + 0.0000207 * X_1 - 0.0000762 * X_2 \quad \text{Eq. 34.}$$

Plots of the predicted values \hat{y}_i vs actual values of profit are shown in Figure 23. Just as in designed experiments prediction model plotting is an integral part of regression model building. The derived regression model in the figure below provides quite good fit to the simulation data. However, some of the values are seemed to be scattered within the figure. Since each of the data points does not lies fairly close to the estimated regression line.

The plot (figure 23) indicates that the variability in profit is increasing as 1st stage pressure (P1) and temperature (T1) increases, which is not exactly a good fit considering the simulation data, for that all the variables should affect the predicted variables of profit. Since, separator 3 was fixed at atmospheric conditions, by having low T1 and high P1, producing as much oil as possible from separator 1. The result suggests that the model used in this work were quite able to identify operating conditions of 1st stage for the profit function in the following section.

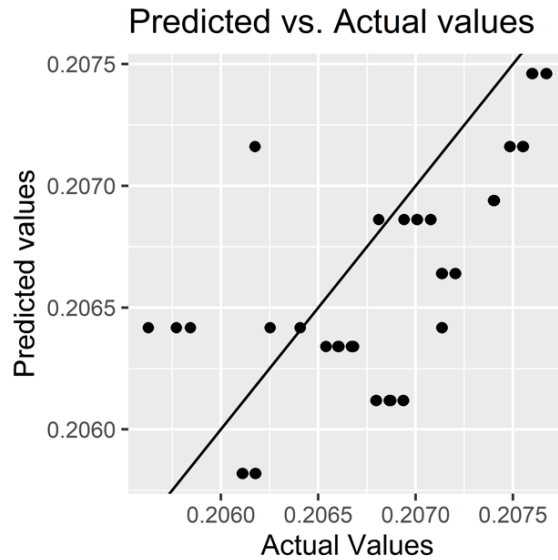


Figure 23: Predicted vs. Actual values of profit.

7.3.2. Statistical output of Response surface methodology

Model fitting

The second order polynomial model used in equation 27 was fitted to the response variable (y), which is Profit. For the corresponding fitting of the explanatory models and the variation of the profit, analyses indicate, that adding terms up to the quadratic significantly improved the model except the interaction effects shown in Table 10 and therefore, it could be the most appropriate model for the response variable.

Regression analysis and ANOVA were used for fitting the RSM model and to check the statistical significance of the terms. The estimated regression coefficients of the quadratic terms for the response variables, along with the corresponding coefficients of the determination R^2 and adjusted- R^2 are given in Table 10, 11 below.

The lack of fit is an implication of the model failure representing the experimental data at which points were not included in the regression or model fluctuations in the model can not be explained by random error (Douglas C. Montgomery, 2008). The response predictor is discarded if there is a significant lack of fit which could be shown by a low probability value. The lack of fit

is shown in the Table 5. did not produce a significant P -value, indicating that these models were adequate for predicting the Profit.

R^2 , coefficients of determination, measures the percentage of variation in the response variable that can be attributed to the model rather than to random error. It was advised that the R^2 should not be less than 85% for a good, fitted model. The lower R^2 indicates that the model is inappropriate for describing the relationship between variables (Barbara M. Beaver & Robert J. Beaver, n.d.). The result output shows that, R^2 values for the response variable were 0.874, which is good, indicating the regression model were suitable to explain the behaviour.

It should be mentioned that whether or not an additional variable is statistically significant, adding it to the model will always increase R^2 . Therefore, a larger value of R^2 does not always indicate the model is adequate. For this reason, it is more suitable to use an adjusted- R^2 of over approx. 90% to evaluate the model adequacy. The result output shows that the adjusted- R^2 for the model is 0.739, which is quite low. Lower adjusted- R^2 suggested that the model contain non-significant terms. Hence, another model has developed to fit the second order polynomial model without the interaction terms as these terms P -value >0.005 to increase the model adequacy has shown in Table 10, which increases the adjusted- R^2 value to 0.808, which is a very good.

The p -value were used as a tool to evaluate the significance of each coefficient. The value is essential to understand the pattern of reciprocal interactions between the test variables. The smaller the magnitude of the p -value the more significant is the corresponding coefficient. P -value <0.005 indicates the terms are significant. From the model of Profit, we can see that, quadratic effects of 1st stage pressure and temperature (P1, T1) were significant (p -value >0.005), and 2nd stage pressure and temperature (P2, T2) were not significant (P -value >0.005) has negative effect on profit function, although the linear term (β_1, β_2) of P1, T1 on profit was significant shown in (Table 11) the ANOVA table below. However, the interaction term ($\beta_{12}, \beta_{13}, \beta_{14}, \beta_{23}, \beta_{24}, \beta_{34}$) was not significant and ($\beta_{13}, \beta_{14}, \beta_{23}, \beta_{24}$) has negative effect on the profit function. For this reason, another model by removing the interaction terms only to make the model better to interpret by achieving little better R^2 value and adjusted R^2 value and p -value of the independent variables.

Table 10: Regression coefficients of the second order polynomial model for the profit (actual values).

Source	Parameters For (Profit milli. \$/day)	P-value	t-value	Significant
Coefficient	0.207808	<0.00000	1130.01	S (***)
Linear				
β_1	0.000409	0.00011	5.45	S (***)
β_2	-0.000415	0.00009	-5.52	S (***)
β_3	0.000071	0.35873	0.95	N
β_4	0.000126	0.11509	1.68	N
Interaction				
β_{12}	0.00004	0.69026	0.40	N
β_{13}	-0.00004	0.69026	-0.40	N
β_{14}	-0.00004	0.69026	-0.40	N
β_{23}	-0.00004	0.69026	-0.40	N
β_{24}	-0.00004	0.69026	-0.40	N
β_{34}	0.00004	0.69026	0.40	N
Quadratic				
β_{11}	-0.00035	0.00047	-4.62	S (***)
β_{22}	-0.00023	0.00920	-3.05	S (**)
β_{33}	-0.00007	0.36702	-0.93	N
β_{44}	-0.00011	0.16043	-1.48	N

Table 11: ANOVA table of the second order polynomial model for the profit (Actual values)

Model	DF	P-value	Significant
Linear (First-order term)	4	0.00006	S (***)
Interaction (Two-way interaction term)	6	0.98152	N
Quadratic term	4	0.00446	S (**)
Residual	13	Total=26 <0.00000	
Lack of fit	10		
Pure error	3		
R^2	0.8746		

Adjusted- R^2	0.7396		
P -value	0.00088		

In next (in Table 12) the first order interaction between the factor investigated are almost as important as their main effects, where the R^2 , adjusted- R^2 , P -value and most importantly the linear and quadratic effect of the model has improved. The relationship between the independent and dependent variables is illustrated in the 3D representation and the corresponding contour plots of the response surface generated by the model. They are most useful approach in terms of visualization of the reaction system at all times where the good fit of the grid obtained to the experimental data can be observed.

The response surface was based on the coefficients represented in Table 13. The data were generated through the four variables at their respective zero level (the centre values of the testing ranges) and the other four were changed within the experimental range. The surface contained by the smallest eclipse in the contour plot represents the maximum predicted value. Generally, the exploration of the response surfaces revealed a complicated interaction between the variables.

The results in Table 12 below indicated that linear and quadratic effect of P1 and T1 were highly significant (for linear: $p < 0.0000$, $p < 0.0000$, for quadratic: $p < 0.0000$, $p < 0.002$) for profit. In addition, 2nd stage temperature (T2) has minor linear and quadratic effect on profit as having $p < 0.063$ or $p < 0.099$. The variables with the largest effect were the linear and quadratic terms of temperature 1st stage followed by the linear terms of pressure, however these variables have no interaction effect with each other. Although pressure at 1st stage increase the profit but slightly high temperature might induce the change the result.

Table 12: Regression coefficients of the second order polynomial model without two-way interaction effect for the profit (actual values of profit).

Source	Parameters For (Profit milli. \$/day)	P -value	t -value	Significant
Coefficient	0.207808	<0.00000	1316.59	S (***)
<i>Linear</i>				

β_1	0.000409	0.00000	6.35	S (***)
β_2	-0.000415	0.00000	-6.44	S (***)
β_3	0.000071	0.28146	1.11	N
β_4	0.000126	0.06389	1.96	S (*)
Quadratic				
β_{11}	-0.00035	0.00003	-5.38	S (***)
β_{22}	-0.00023	0.00209	-3.56	S (**)
β_{33}	-0.00007	0.28980	-1.09	N
β_{44}	-0.00011	0.09903	-1.73	S (*)

At higher P2 did not have much effect on the profit function while at slightly higher T2 slightly increase the profit. Hence, conclusions can only be drawn if the influence of these variables on the response variable (profit) is studied in considering all.

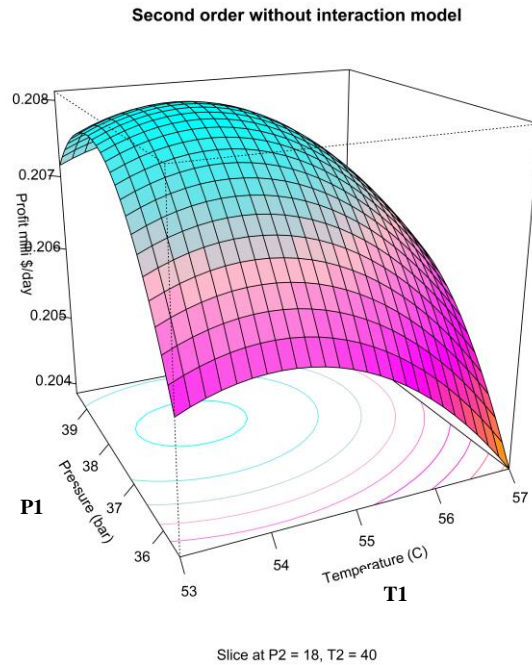
Table 13: ANOVA table of the second order polynomial model without Two-way interaction model for the profit (Actual values).

Model	DF	P-value	Significant
Linear (First-order term)	4	0.00000	S (***)
Quadratic term	4	0.00036	S (**)
Residual	19	Total=38	
Lack of fit	16		<0.00000
Pure error	3		
R^2	0.865		
Adjusted- R^2	0.808		
P-value	0.00000		

Profit function

The variation of profit function with 1st stage and 2nd stage temperature and pressure is presented in Figure 24 a. And b below. As it shows, the profit increases exponentially with temperature and pressure. Higher temperatures at 1st stage, profit decreases because of less oil production. The effect of pressure was more pronounced at lower temperature.

a)



b)

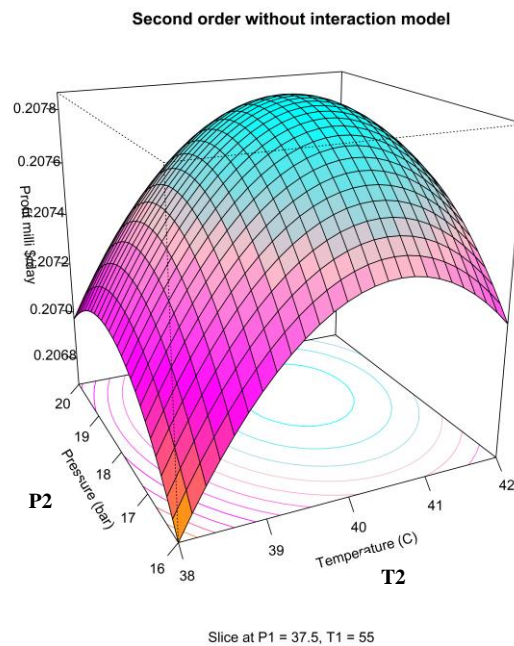


Figure 24: Response surface for the effect of (a. T_1 and P_1 on Profit function), (b. T_2 and P_2 on profit function).

In addition, the profit reached nearly the equilibrium towards the temperature but at higher temperature did not have much effect on profit. However, when 1st stage temperature and pressure

was kept at mid level (intermediate level) increase of T2 is the main reason for an exponential increase in the profit. This is due to the more availability of the oil at that operating condition which increases the driving force of profit of the oil and gas production.

Effect of P2 on profit was minor. Based on the study, the optimal conditions for maximum profit were given by the RSM (Response surface methodology) model: P1 = 38.08 bar, T1=54.09°C, P2=18 bar, T2=40.56°C and profit (y) = 0.208 milli. \$/day.

7.3.3. Optimal Conditions

The range of optimum condition was determined by the contour plot of the response value (profit) Figures 25.a and Figure.b represent the contour plots for the response which were evaluated as function of 1st and 2nd stage pressure and temperature. In fact, this is a typical example, where the main effect of P1(β_1) and T1(β_2) (shown in figure 25.a) and P2(β_3) and T2(β_4) (shown in figure 25.b) seems to indicate that the profit is sensitive to the variation of P1, T1, P2 and T2. This is only true at high P1 whereas at low P1, the profit is decreasing with decreasing T1, because of might be in separator 1 of the process oil production is higher. A relatively modest quadratic effect is observed as P1-P1(β_{11}), T1-T1(β_{22}), and T2-T2(β_{34}), whereas P2-P2(β_{33}) was not a significant factor as shown in Table 13, due to the fact that the P2(β_3) does not effect to the maximum oil and gas production. In figure 25.a and b. we can see as P2 decreases, but T2 (°C) increases profit becomes higher, where it got its stationary point.

A small white shaded area, namely saddle area in the middle of the plot of the response variable is assigned as the optimum point that represents a higher amount of profit that can be achieved out of oil and gas sales using the best combinations of 1st and 2nd stage pressure and temperature. The saddle is appropriate apparent for P1(bar) and T1 (°C), and for P2 (bar) and T2 (°C) and the response surface indicates that the stationary point was at maximum point.

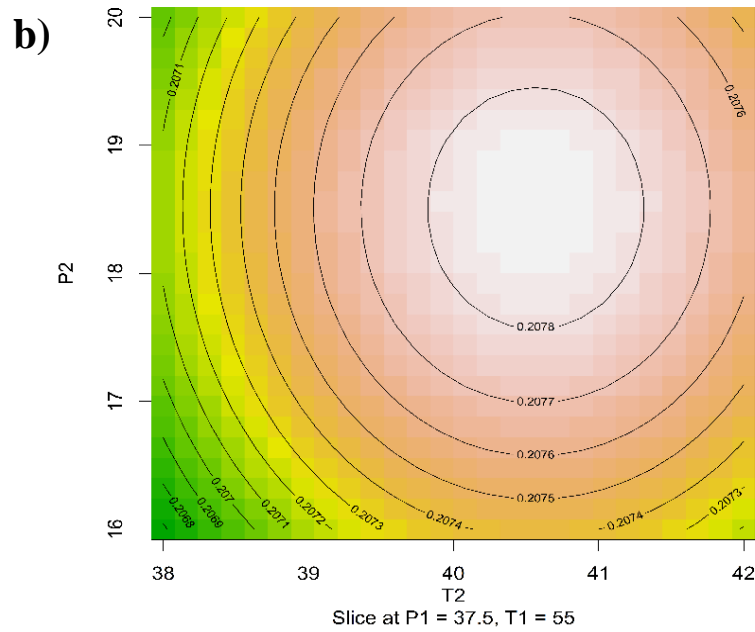
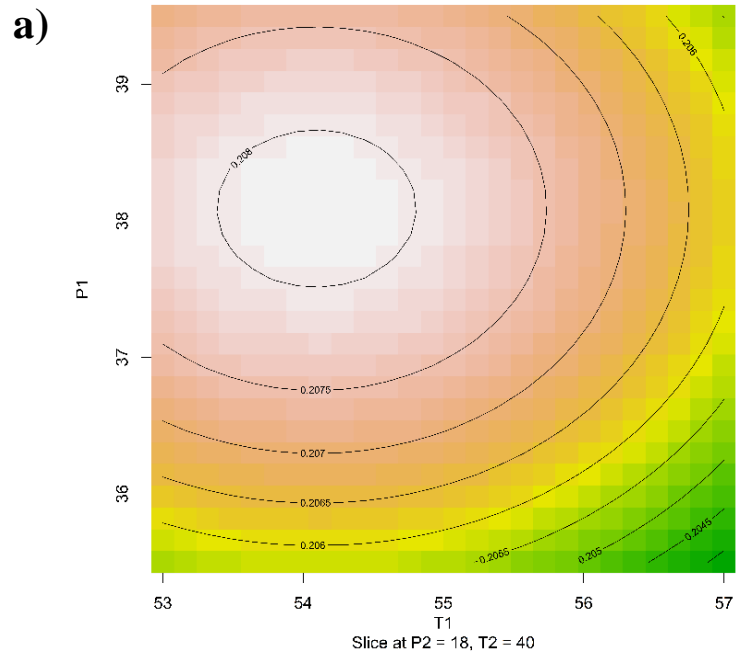


Figure 25: The optimum region by the saddle point in the contour plot for profit evaluated as function of (a. 1st stage pressure, $P1 = 38.08$ bar and temperature, $T1 = 40.56^\circ\text{C}$), (b. 2nd stage pressure, $P2 =$ and temperature, $T2 = 40.56^\circ\text{C}$).

The stationary point of response surface is at $X_1 = 0.5893$, $X_2 = -0.9048$, $X_3 = 0.0000$, and $X_4 = 0.5672$ which indicates that, stationary point in original points of the figures where $P1 = 38.08$ bar, $T1 = 54.09^\circ\text{C}$, $P2 = 18.00$ bar, and $T2 = 40.57^\circ\text{C}$.

Hence, these two plots illustrate, the determination of best combinations factors at $P1 = 38.08$ bar, $T1 = 54.09^\circ\text{C}$, $P2 = 18$ bar, $T2 = 40.56^\circ\text{C}$ on profit of oil and gas sales as the best combinations. Therefore, we can say that the saddle point shows that the optimal conditions of maximum oil and gas production leading to maximum profit within the experimental data, as predicted by the model (second order model without interaction term), were at 0.208 milli \$/day. Therefore, using an optimum operating condition of $P1 = 38.08$ bar, $T1 = 54.09^\circ\text{C}$, $P2 = 18.00$ bar and $T2 = 40.56^\circ\text{C}$ we can have 0.208 milli \$/day profit out of the oil and gas sales.

7.4. Summary

Response surface methodology (RSM) can be useful tool to find out the optimum temperature and pressure for optimizing the oil and gas facilities. The multiple regression model closely reflects the process simulations result. Despite the high complexity of the process simulations, which includes a large number of different unit operations to represent, the multiple regression model quite adequately captures these impacts. More importantly, RSM can be great tool for optimizing oil and gas separation facilities by maximizing the profit milli. \$/day. The most important parameter that affect the profit function is that the Pressure and temperature at 1st stage and temperature at 2nd stage.

Chapter 8: Conclusion and future work

This chapter represents the conclusions of the current work and the suggestion of research activities in the future of this work.

8.1. Conclusion

In this study a separation train design of oil and gas separation is conducted using Aspen HYSYS V9.0 software to investigate the effect of different operating conditions on oil and gas production.

A literature study on separator modelling in offshore oil and gas plant was performed and then in next a consecutive study on thermodynamic analysis was elaborated, in which a vapor liquid equilibrium calculation was chosen to model the separators. This model used the Peng-Robinson equation of state. The vapor liquid equilibrium calculation was implemented through choosing a thermodynamic package (Peng-Robinson EOS) which was built in Aspen HYSYS, which efficiently separates the well fluid into the two phases of vapor and liquid.

First, the separation train design was built with three stages along with two compressors was used to show that the recovery of intermediate components (C_3 , C_4 , C_5) while maintaining its stability was dependent on the separator pressure and temperature and the reservoir fluid composition. This example demonstrated that adaptive separator pressure and temperature could increase the oil and gas production and income from oil and gas sales using an objective function. In addition, energy consumption was low within producing maximizing the oil and gas production, but consumption was little higher in compressor 2 compared to compressor 1.

Determining an optimum operating point this study proposed a optimization method, which is Response surface methodology (RSM). RSM uses a second-order polynomial algorithm without the two-way interaction terms to find out the maximum profit value. To perform that, Central composite design (CCD) was applied by creating (High, low, centre level) coded variable of actual operating variables to be tested and the profit was increased with 0.208 milli \$/day at optimum operating point where $P_1 = 38.08$ bar, $T_1 = 54.09^\circ\text{C}$, $P_2 = 18.00$ bar and $T_2 = 40.56^\circ\text{C}$. Therefore,

good agreement between the predicted and measured data (simulation data) at the predicted optimal conditions confirmed the usefulness of the model.

8.2. Future work

Overall Response surface methodology (RSM) showed to be robust and promising tool to find the optimum operating point of pressure and temperature for the maximum profit value. A highly significant (p -value <0.001) statistical model was obtained from analysis of the data through RSM. The largest effect was for P1 (bar), T1 (°C) and T2 (°C) respectively. But the interaction effects that leads to the subsequent generation of set of regression equations were not significant and P2 (bar) was not significant having (p -value). With considering maximum oil and gas production the maximum profit value was obtained at P1 = 38.08 bar, T1 = 54.09°C, and T2 = 40.56°C, where the P2 = 18 bar did not change at all, which refers to use more efficient operating parameters for P2 which does affect on the maximum profit value.

Furthermore, in this study the separation performance is considered as an indicator to explain the effect of temperature and pressure on hydrocarbon recovery and stabilization of oil and gas components and the assessment of the optimization results. In future, the result from the present study is that one should never focus only on finding the optimum operating pressure and temperature when finding the maximum profit value, but also the minimum energy consumption. One should always consider using a plant wide optimization approach and consider the entire process. There is a strong interplay between the process variables, which offers both some complexity, but obviously also increases the number of process variables that needs to be tuned.

Appendix 1:

Table 14: Process simulation responses to coded variable build using CCD. 1=high value, 0= mid value and -1= low value.

X1	X2	X3	X4	P1	T1	P2	T2	Profit
-1	-1	-1	-1	25	50	12	30	0.20665
1	-1	-1	-1	50	50	12	30	0.20744
-1	1	-1	-1	25	60	12	30	0.20580
1	1	-1	-1	50	60	12	30	0.20659
-1	-1	1	-1	25	50	24	30	0.20679
1	-1	1	-1	50	50	24	30	0.20758
-1	1	1	-1	25	60	24	30	0.20594
1	1	1	-1	50	60	24	30	0.20673
-1	-1	-1	1	25	50	12	45	0.20701
1	-1	-1	1	50	50	12	45	0.20770
-1	1	-1	1	25	60	12	45	0.20779
1	1	-1	1	50	60	12	45	0.20615
-1	-1	1	1	25	50	24	30	0.20694
1	-1	1	1	50	50	24	45	0.20775
-1	1	1	1	25	60	24	45	0.20793
1	1	1	1	50	60	24	45	0.20708
-2	0	0	0	20	55	18	40	0.20567
2	0	0	0	60	55	18	40	0.20773
0	-2	0	0	37.5	45	18	40	0.20780
0	2	0	0	37.5	65	18	40	0.20654
0	0	-2	0	37.5	55	8	40	0.20780
0	0	2	0	37.5	55	28	40	0.20774
0	0	0	-2	37.5	55	18	25	0.20754
0	0	0	2	37.5	55	18	50	0.20780
0	0	0	0	37.5	55	18	40	0.20780
0	0	0	0	37.5	55	18	40	0.20780
0	0	0	0	37.5	55	18	40	0.20780
0	0	0	0	37.5	55	18	40	0.20780

References

- Adamczyk, J., Horny, N., Tricoteaux, A., Jouan, P. Y., & Zadam, M. (2008). On the use of response surface methodology to predict and interpret the preferred c-axis orientation of sputtered AlN thin films. *Applied Surface Science*, 254(6), 1744–1750. <https://doi.org/10.1016/j.apsusc.2007.07.139>
- Ahmed, T. (2007). *Equations of State and PVT Analysis: Applications for Improved Reservoir Modeling*. Houston: Gulf Publishing Company.
- Andreasen, A. (2020). Applied process simulation-driven oil and gas separation plant optimization using surrogate modeling and evolutionary algorithms. *ChemEngineering*, 4(1), 1–21. <https://doi.org/10.3390/chemengineering4010011>
- Andreasen, A., Rasmussen, K. R., & Mandø, M. (2018). Plant Wide Oil and Gas Separation Plant Optimisation using Response Surface Methodology. *IFAC-PapersOnLine*, 51(8), 178–184. <https://doi.org/10.1016/j.ifacol.2018.06.374>
- ARNOLD, K., & STEWART, M. (1998). *Design of oil-handling systems and facilities*. Gulf Professional Publishing, 1998.
- Bahadori, A., Vuthaluru, H. B., & Mokhatab, S. (2008). Optimizing separator pressures in the multistage crude oil production unit. *Asia-Pacific Journal of Chemical Engineering*, 3(4), 380–386. <https://doi.org/10.1002/apj.159>
- Barbara M. Beaver, & Robert J. Beaver. (n.d.). *Introduction to Probability and Statistics* (15th ed.).
- Becker, F. G., Cleary, M., Team, R. M., Holtermann, H., The, D., Agenda, N., Science, P., Sk, S. K., Hinnebusch, R., Hinnebusch A, R., Rabinovich, I., Olmert, Y., Uld, D. Q. G. L. Q., Ri, W. K. H. U., Lq, V., Frxqwu, W. K. H., Zklfk, E., Edvhg, L. V, Wkh, R. Q., ... ح. فاطمی. (2015). No 主観的健康感を中心とした在宅高齢者における健康関連指標に関する共分散構造分析
- Bidgoli, A. A. (2020). *Simulation and optimization of primary oil and gas processing plant of FPSO operating in pre-salt oil field*. <http://dx.doi.org/10.11606/t.3.2018.tde-13122018-150547%0Ahttp://www.teses.usp.br/teses/disponiveis/3/3150/tde-13122018-150547/publico/AliAllahyarzadehBidgoliCorr18.pdf>
- Bin Dainure, M. F. (2013). *Process Simulation of Crude Oil Stabilization System: An Industrial Case Study*. May, 1–105.
- Box G. E. P. and Wilson, K. B. (1992). On the Experimental Attainment of Optimum Conditions. In N. L. Kotz Samueland Johnson (Ed.), *Breakthroughs in Statistics: Methodology and Distribution* (pp. 270–310). Springer New York. https://doi.org/10.1007/978-1-4612-4380-9_23
- Courses, M., Supervisor, E., Solbraa, E., & Iliopoulos, E. S.-. (2019). *Optimisation of offshore oil and gas processing plants based on online cricondenbar and TVP analysis*. June.
- Douglas C. Montgomery. (2008). *Design and Analysis of Experiments*. John Wiley & Sons.
- Elgsæter, S. M., Slupphaug, O., & Johansen, T. A. (2010). A structured approach to optimizing offshore oil and gas production with uncertain models. *Computers and Chemical Engineering*, 34(2), 163–176. <https://doi.org/10.1016/j.compchemeng.2009.07.011>

- Gaganis, V., & Varotsis, N. (2014). An integrated approach for rapid phase behavior calculations in compositional modeling. *Journal of Petroleum Science and Engineering*, 118, 74–87. <https://doi.org/10.1016/J.PETROL.2014.03.011>
- Ghaedi, M., Ebrahimi, A. N., & Pishvaie, M. R. (2014a). APPLICATION OF GENETIC ALGORITHM FOR OPTIMIZATION OF SEPARATOR PRESSURES IN MULTISTAGE PRODUCTION UNITS. *Chemical Engineering Communications*, 201(7), 926–938. <https://doi.org/10.1080/00986445.2013.793676>
- Ghaedi, M., Ebrahimi, A. N., & Pishvaie, M. R. (2014b). APPLICATION OF GENETIC ALGORITHM FOR OPTIMIZATION OF SEPARATOR PRESSURES IN MULTISTAGE PRODUCTION UNITS. *Chemical Engineering Communications*, 201(7), 926–938. <https://doi.org/10.1080/00986445.2013.793676>
- Handbook of Statistical Methods*. (2012). NIST/SEMATECH e.
- Hu, X. (2017). *The Physical Properties of Reservoir Fluids*. https://doi.org/10.1007/978-3-662-53284-3_3
- Julian J. Faraway. (2004). *Linear Models with R*. CRC Press.
- Kamışlı, F., & Ahmed, A. A. (2019). *Simulation and Optimization of A Crude Oil Distillation Unit Ham Petrol D amıtma Ünitesinin Simülasyonu ve Optimizasyonu*. 14(2), 59–68.
- Kim, I. H., Dan, S., Kim, H., Rim, H. R., Lee, J. M., & Yoon, E. S. (2014). Simulation-based optimization of multistage separation process in offshore oil and gas production facilities. *Industrial and Engineering Chemistry Research*, 53(21), 8810–8820. <https://doi.org/10.1021/ie500403a>
- Koocheiki, A., Taherian, A. R., Razavi, S. M. A., & Bostan, A. (2009a). Response surface methodology for optimization of extraction yield, viscosity, hue and emulsion stability of mucilage extracted from *Lepidium perfoliatum* seeds. *Food Hydrocolloids*, 23(8), 2369–2379. <https://doi.org/10.1016/j.foodhyd.2009.06.014>
- Koocheiki, A., Taherian, A. R., Razavi, S. M. A., & Bostan, A. (2009b). Response surface methodology for optimization of extraction yield, viscosity, hue and emulsion stability of mucilage extracted from *Lepidium perfoliatum* seeds. *Food Hydrocolloids*, 23(8), 2369–2379. <https://doi.org/10.1016/j.foodhyd.2009.06.014>
- Kylling, Ø. (2009). *Optimizing separator pressure in a multistage crude oil production plant*. June, 86. <http://ntnu.diva-portal.org/smash/record.jsf?pid=diva2:347760>
- Ling, K., Wu, X., Guo, B., & He, J. (2013). New Method To Estimate Surface-Separator Optimum Operating Pressures. *Oil and Gas Facilities*, 2(03), 65–76. <https://doi.org/10.2118/163111-PA>
- Neto, A. M. B., & Bannwart, A. C. (2015). PVTpetro : A COMPUTATIONAL TOOL FOR ISOTHERM TWO- PHASE PT-FLASH CALCULATION IN OIL-GAS SYSTEMS. *Congresso Brasileiro de Engenharia Química, 2015*, 1–8.
- Pasquale, A. P. (2007). *Optimization of Offshore Oil & Gas Separation Train*.
- Qadri, S., Saleh, M., Qadri, S., & Saleh, M. (2020). *Effect of Physical Factors on Separation Efficiency of GAS From Oil Case Study in Alif Oil Field (Block 18)*. 17(1).
- Qiu, L., Wang, Y., Jiao, Q., Wang, H., & Reitz, R. D. (2014). Development of a thermodynamically consistent, robust and efficient phase equilibrium solver and its validations. *Fuel*, 115, 1–16. <https://doi.org/10.1016/J.FUEL.2013.06.039>
- Rachford, H. H., & Rice, J. D. (1952). Procedure for Use of Electronic Digital Computers in Calculating

Flash Vaporization Hydrocarbon Equilibrium. *Journal of Petroleum Technology*, 4(10), 19–3.
<https://doi.org/10.2118/952327-G>

Speight, & James G. (2014). *Handbook of offshore oil and gas operation*.

Statistics, M. (2016). *Multi-Factor Experimental Designs for Exploring Response Surfaces* Author (s): G . E . P . Box and J . S . Hunter Source : *The Annals of Mathematical Statistics* , Vol . 28 , No . 1 (Mar . , 1957) , pp . 195-241 Published by : Institute of Mathematical St. 28(1), 195–241.

Sutherland, K. (2012). Separation processes in oil and gas extraction. *Filtration and Separation*, 49(1), 20–25. [https://doi.org/10.1016/S0015-1882\(12\)70054-X](https://doi.org/10.1016/S0015-1882(12)70054-X)

Willersrud, A., Imsland, L., Hauger, S. O., & Kittilsen, P. (2013). Short-term production optimization of offshore oil and gas production using nonlinear model predictive control. *Journal of Process Control*, 23(2), 215–223. <https://doi.org/10.1016/j.jprocont.2012.08.005>